New insights into widely linear MMSE receivers for communication networks using data-like rectilinear or quasi-rectilinear signals -Part I: one and two-inputs receivers

Pascal Chevalier, Jean-Pierre Delmas, Roger Lamberti

New insights into widely linear MMSE receivers for communication networks using data-like rectilinear or quasi-rectilinear signals - Part I: one and two-inputs receivers

Pascal Chevalier, Jean-Pierre Delmas, and Roger Lamberti

***Abstract*—Widely linear (WL) processing has been of great interest these last two decades for multi-user (MUI) interference mitigation in radiocommunications networks using rectilinear (R) or quasi-rectilinear (QR) signals in particular. Despite numerous papers on the subject, this topic remains of interest for several current applications which use R or QR signals such as anti-collisions in Radio Frequency Identification (RFID) or satellite-AIS systems, for grant free massive access in NB-IOT networks, for multipaths mitigation in the Control and Non Payload Communications (CNPC) link of Unmanned Aerial Vehicle (UAV) or FBMC-OQAM networks. In this context, the purpose of this paper, and the companion paper [50], is to get new insights into WL MMSE receivers for communication networks using R or QR signals, aiming in particular at discarding the need to estimate the MUI channels for their implementation, always cumbersome in practice, while keeping their MMSE optimality. For this purpose, several WL MMSE receivers, with and without any structure constraint, exploiting or not the cyclostationarity properties of the signals, are considered in this paper and [50] and their performance are computed and compared, both analytically and by computer simulations, for R and QR signals in the absence and in the presence of one MUI. Several new enlightening results are obtained, for two-input WL MMSE receiver in this paper, and three-input WL MMSE receivers in [50], showing in particular the non-equivalence of R and QR signals for WL MMSE receivers. Moreover, the conditions under which WL MMSE receivers discard the need to estimate the MUI channels while preserving MMSE optimality are given. These results are very useful for implementation issues optimization in particular.**

***Index Terms*—Non circular, widely linear, MMSE, rectilinear, quasi-rectilinear, SAIC/MAIC, MUI, MAI, ISI, ICI, continous-time, FRESH, GMSK, OQAM, ASK, PSK, QAM, Beyond5G, AIS, FBMC, UAV, CNPC.**

P. Chevalier is with CNAM, laboratoire CEDRIC, HESAM University, 292 rue Saint Martin, 75141 Paris Cedex 3, France and also with Thales France, HTE/AMS/TCP, 4 Av. Louvresses, 92622 Gennevilliers, Cedex, France e-mail: pascal.chevalier@cnam.fr, pascal.chevalier@thalesgroup.com.

J.-P. Delmas is with Samovar laboratory, Telecom SudParis, Institut Polytechnique de Paris, 91120 Palaiseau, France, e-mail: jean-pierre.delmas@it-sudparis.eu.

R. Lamberti is with CITI department, Telecom SudParis, Institut Polytechnique de Paris, 91120 Palaiseau, France, e-mail: roger.lamberti@mines-telecom.fr.

Paper submitted to IEEE Trans. Vehicular Technology

I. Introduction

WIDELY linear (WL) processing [1] has been of great interest these last two decades for many applications involving second-order (SO) non-circular (or improper) signals [2] and for multi-user interference (MUI) and multi-antenna interference (MAI) mitigation in radiocommunication networks using rectilinear (R) or quasi-rectilinear (QR) modulations in particular. Let us recall that R modulations correspond to mono-dimensional modulations such as amplitude modulation (AM), amplitude shift keying (ASK) or binary phase shift keying (BPSK) modulations, whereas QR modulations are complex modulations corresponding, after a simple derotation operation [3], to a complex filtering of a R modulation. Examples of QR modulations are $\pi/2$-BPSK, minimum shift keying (MSK) or offset quadrature amplitude (OQAM) modulations, while an example of approximated QR modulation is the Gaussian MSK (GMSK) modulation.

More precisely, WL processing has been considered in the past for R MUI and narrow-band interference (NBI) mitigation in code division multiple access (CDMA) networks [4]–[11], in orthogonal frequency division multiplex systems [12] and in ultra wide band networks [13] in particular. It has also been proposed for R MAI suppression in V-BLAST single user Muti-Input Multi-Output (MIMO) systems [14], [15] and for R MUI mitigation in MIMO systems using spatio-temporal block coding [16]. Moreover, since the end of the nineties, WL processing has also been proposed for QR MUI mitigation in CDMA networks using offset quadrature phase shift keying (OQPSK) modulation [17]. It has also been strongly studied and applied for single/multiple antenna interference cancellation (SAIC/MAIC) in radiocommunication networks using QR signals, and in the GSM cellular networks in particular, which use the GMSK modulation. Several SAIC WL receivers, allowing the separation of two users from only one receive antenna, have been proposed in [18]–[21] and inserted in most of GSM

handsets since 2006 [22], allowing significant capacity gains in GSM networks [20], [23]. Other WL receivers have also been proposed for SAIC [24]–[26] and SAIC/MAIC [27] in voice services over adaptive multi-user channels on one slot (VAMOS) networks, a standardized extension of GSM networks, aiming at increasing the capacity of GSM, while maintaining backward compatibility with the legacy system.

Despite these numerous papers about WL processing for R and QR MUI or MAI mitigation, this topic remains of great interest for several current and future applications. This concerns in particular anti-collisions processing in radio frequency identification systems [28] or in dense machine-type networks such as grant-free narrow-band internet of things (IoT) networks for uplink transmissions [29], which use R and QR signals respectively, and in satellite-AIS systems for maritime surveillance which use GMSK signals [30]–[32]. This topic is also relevant to allow 5G and beyond 5G (B5G) networks to support a massive number of low data rate devices through one-dimensional signaling [33], [34], potentially jointly with MIMO non-orthogonal multiple access (MIMO-NOMA) systems [35], or fully or over-loaded large MU-MIMO systems using R signals [36]. Moreover, QR interference mitigation by WL processing remains also of great interest for unmanned aerial vehicles (UAVs or drones), who are expected to become one of the important enabling technologies for B5G cellular networks and whose applications development is growing dramatically for many civilian applications (monitoring, surveillance, traffic control, relaying etc..) [37], [38]. Indeed, the bidirectional Control and Non Payload Communications (CNPC) link, connecting the ground control station to the UAV, which is a safety-critical link requiring improved receivers in terms of reliability, availability and low latency in a large variety of environmental and propagation conditions, uses the GMSK modulation [39]. In low-altitude operations, CNPC links meet frequency selective wireless channels and WL processing is of interest for channel equalization, as already described recently in [40]. In order to reduce the size, and then the complexity, of the equalizer, an additional interest of WL processing may be to potentially cancel the multiple paths arriving outside the equalizer length, thus considered as MUI. Another application where QR interference mitigation by WL processing may be still of interest concerns communication networks using FBMC-OQAM waveforms [41] candidate for beyond 5G and future Internet of Things networks [42], thanks to their good frequency localization and compatibility with asynchronous links. For frequency selective channel, FBMC-OQAM waveforms generate Inter-Carrier Interference (ICI) at reception, which may be processed by efficient WL processing. Preliminary WL based solutions for FBMC-OQAM waveforms are presented in [43]–[45] for MIMO links using spatial multiplexing at transmission and in [46], [47] for SISO links.

In this challenging context, let us note that most of the WL receivers currently available in the literature for R or QR MUI, MAI or ICI mitigation are WL MMSE receivers [4]–[7], [9], [10], [12]–[17], [19]–[21], [24]–[29], [33], [36], [43]–[47]. Although these receivers have been strongly studied these two last decades, several important questions related to their structure, performance, implementation and potential equivalence for R and QR signals remain surprisingly raised. Indeed, all the previous WL MMSE receivers, except those presented in [17] and [27], are implemented at the symbol rate, after a matched filtering operation to the pulse shaping filter, and have thus a particular structure constraint, which is shown in this paper to be sub-optimal in many situations and for frequency selective channels in particular. However, the impact on the performance of this structure constraint does not seem to have been precisely analysed and quantified in the literature for arbitrary frequency selective channels or in the presence of MUI, which may prevent to implement potential more powerful WL MMSE receivers. In addition, some of these WL MMSE receivers [14], [15], [28], [29], [33], [36], [43], [44] fully exploit the similar waveform of SOI and MUI by jointly estimating the SOI and interference symbols, which requires the a priori knowledge or estimation of both the SOI and interference channels. Other WL MMSE receivers [4]–[7], [9], [10], [12], [13], [19]–[21], [24]–[27], [45]–[47] estimate the SOI symbols only, which does not require the a priori knowledge or estimation of the interference channels. Nevertheless, up to the best of our knowledge, performance of these two approaches, both without and with the previous structure constraint, do not seem to have been compared to each other, which potentially prevent joint receivers from discarding the need of interference channel estimation, always cumbersome in practice. Moreover, in most of the previous papers which consider QR signals, after a derotation operation, QR signals are processed as R ones, and seem to be considered equivalent to the latter, despite the fact that it has been proved recently [48], [49], through a pseudo-MLSE approach, that QR and R signals are generally not equivalent for WL processing due to their different SO cyclostationary properties. For this reason, three-input WL frequency shift (FRESH) receivers have been proposed in [48] and [49] for QR signals, without and with frequency-offsets respectively, to make them almost equivalent to R ones for pseudo-MLSE WL processing. One may then wonder whether this non equivalence between R and QR signals remains true for WL MMSE receivers and whether the concept of three-input WL FRESH receiver for QR signals may also be interesting or useful for WL MMSE approaches.

The purpose of this paper, and the companion one [50], is to get new insights into WL MMSE receivers for communication networks which use R or QR signals. This is done by bringing answers to all the previous important questions, crucial for performance and practical implementation

optimizations in particular, and by proposing new powerful alternative receivers easier to implement. More precisely, we consider in this paper a R or a QR SOI which propagates through an arbitrary frequency selective channel and which is received by an array of antennas. This SOI is corrupted by data-like MUI (or MAI) and background noise. For each kind of SOI (R or QR), we derive in a first step, several L (or one-input) and WL (or two-input) MMSE receivers, either without or with the structure constraint of the literature, exploiting or not the full knowledge of MUI waveform. To do so, we adopt a continuous-time (CT) approach which is justified by three reasons. The first one, is that implementation issues are out of the scope of the paper, which is mainly conceptual but which may be a prerequisite for implementation optimizations investigated elsewhere. The second one, is that a CT approach allows us to remove the potential influence of the sample rate imposed by a discrete-time (DT) approach. The third one, is that it allows us to obtain analytical and potentially interpretable expressions for the output performance of the receivers considered in the paper, which are completely original. Concerning the considered MMSE receivers, let us recall that the optimal L and WL MMSE receivers have no structure constraint and fully exploit the MUI waveform knowledge. In other words, they implicitly exploit all the cyclostationary properties of the MUI, in addition to their SO non-circularity for optimal WL MMSE receiver. As a consequence, MMSE receivers having a particular structure constraint or which do not fully exploit the MUI waveform knowledge, by assuming them falsely stationary for example, are generally sub-optimal. This is in particular the case for most of L and WL MMSE receivers of the literature, which are implemented at the symbol rate, after a matched filtering operation to the pulse shaping filter and which prevent from exploiting the SO cyclostationarity property of MUI. In a second step, we give closed-form expressions of the Signal to Interference plus Noise ratio (SINR) on the current symbol at the real-part output of all the considered receivers and we develop very insightful analytical interpretable expressions of these SINRs in some particular cases, which is very original. In a third step we compare the performance of all the computed receivers, for several kinds of signals, and derive conditions under which the considered receivers are equivalent or not. We show in particular several new interesting results about L and two-input WL MMSE receivers, which may be very useful for practical implementations issues, analysed elsewhere. The first result is the sub-optimality of most of the MMSE receivers of the literature for frequency selective channels. The second result is the equivalence, both without any structure constraint and with the structure constraint of the literature, of WL MMSE receivers estimating the SOI symbols either solely or jointly with those of the MUI, provided that the MUI waveform knowledge is fully exploited. For receivers without any structure constraint, the third result is the general non-equivalence of WL MMSE receivers fully exploiting or not the MUI waveform knowledge. The fourth result is the general non-equivalence of R and QR signals for two-input WL MMSE receivers in the presence of MUI. Without any structure constraint and for R signals, the fifth result is the increasing quasi-optimality, as the bandwidth of the signals decreases, and the increasing sub-optimality, as the latter increases, of two-input WL MMSE receiver which does not fully exploit the MUI waveform knowledge by falsely assuming MUI to be stationary. For R signals, this discards the need in practice, at least for decreasing bandwidths, to estimate the MUI channel without discarding the practical MMSE quasi-optimality. This result can be extended to QR signals provided that three-input WL FRESH MMSE receivers are considered instead of two-input ones, as shown in the companion paper [50], where other results are also presented, for both R and QR signals.

The paper is organized as follows. Section II introduces the observation model and the extended one for standard two-input WL processing of both R and QR signals, jointly with the SO statistics of the total noise. Section III derives, for R and QR signals, the L and standard two-input WL MMSE receivers, without and with a structure constraint, fully exploiting or not the MUI waveform knowledge. Section IV gives general closed-form expressions of the SINR on the current symbol at the real-part output of these derived receivers, for R and QR signals, and gives engineering insights and comparative analysis of these SINR for several propagation channels, and several kinds of signals, in the presence of zero and one MUI. Symbol Error Rate (SER) analysis and illustrations will be presented in [50] due to lack of place. Finally section V concludes this paper.

Notations: Before proceeding, we fix the notations used throughout the paper. Non boldface symbols are scalar whereas lower (upper) case boldface symbols denote column vectors (matrices). T, H and $*$ means the transpose, conjugate transpose and conjugate, respectively. $\otimes$ is the convolution operation. $\delta(x)$ is the Kronecker symbol such that $\delta(x) = 1$ for $x = 0$ and $\delta(x) = 0$ for $x \neq 0$. $\mathbf{0}_K$ and $\mathbf{I}_K$ are the zero and the identity matrices of dimension K, respectively and $\mathbf{J}_{2K}$ is the $2K \times 2K$ exchange matrix. Moreover, all Fourier transforms of vectors $\mathbf{x}$ and matrices $\mathbf{X}$ use the same notation where time parameters t or τ is simply replaced by frequency f.

II. Models and total noise second-order statistics

A. Observation model and total noise SO statistics

A1) *Observation model:* We consider an array of N narrow-band antennas receiving the contribution of a SOI, which may be R or QR, P data-like MUI, having the same nature (R or QR), the same symbol period and the same pulse-shaping filter as the SOI, and a background noise. The $N \times 1$ vector of complex amplitudes of the data at the output

of these antennas after frequency synchronization can then be written as

$$\begin{aligned}\mathbf{x}(t) &= \sum_{\ell} a_\ell \mathbf{g}(t-\ell T) + \sum_{1\le p\le P}\sum_{\ell} a_{p,\ell}\mathbf{g}_p(t-\ell T)+\boldsymbol{\epsilon}(t) \\ &= \sum_{\ell}\mathbf{G}(t-\ell T)\mathbf{a}_\ell+\boldsymbol{\epsilon}(t) \stackrel{\text{def}}{=} \sum_{\ell} a_\ell \mathbf{g}(t-\ell T)+\mathbf{n}(t) \quad (1)\end{aligned}$$

Here, $(a_\ell, a_{p,\ell}) = (b_\ell, b_{p,\ell})$ for R signals, whereas $(a_\ell, a_{p,\ell}) = (j^\ell b_\ell, j^\ell b_{p,\ell})$ for QR signals, where b_ℓ and $b_{p,\ell}$ $(1 \le p \le P)$ are real-valued zero-mean independent identically distributed (i.i.d.) random variables, corresponding to the SOI and MUI p symbols respectively for R signals and directly related to the SOI and MUI p symbols, respectively for QR signals [51]–[53], T is the symbol period for R, $\pi/2$-BPSK, $\pi/2$-ASK, MSK and GMSK signals [52], [53] and half the symbol period for OQAM signals [51], $\mathbf{g}(t) = v(t) \otimes \mathbf{h}(t)$ is the $N \times 1$ impulse response vector of the SOI global channel, $v(t)$ and $\mathbf{h}(t)$ are respectively the scalar and $N \times 1$ impulse responses of the SOI pulse shaping filter and propagation channel, respectively, $\mathbf{g}_p(t) \stackrel{\text{def}}{=} v(t) \otimes \mathbf{h}_p(t)$ where $\mathbf{h}_p(t)$ is the impulse response vector of the propagation channel of the MUI p, $\mathbf{G}(t)$ is the $N \times (P+1)$ matrix defined by $\mathbf{G}(t) \stackrel{\text{def}}{=} [\mathbf{g}(t), \mathbf{g}_1(t), ..., \mathbf{g}_p(t)] = v(t) \otimes \mathbf{H}(t)$ where $\mathbf{H}(t) \stackrel{\text{def}}{=} [\mathbf{h}(t), \mathbf{h}_1(t), ..., \mathbf{h}_p(t)]$, $\mathbf{a}_\ell$ is the $(P+1)\times 1$ vector defined by $\mathbf{a}_\ell \stackrel{\text{def}}{=} [a_\ell, a_{1,\ell}, ..., a_{P,\ell}]^T$, $\boldsymbol{\epsilon}(t)$ is the $N \times 1$ background noise vector assumed to be zero-mean, circular, stationary, temporally and spatially white and $\mathbf{n}(t)$ is the total noise vector composed of the P MUI and background noise. Note that model (1) with $(a_\ell, a_{p,\ell}) = (j^\ell b_\ell, j^\ell b_{p,\ell})$ is exact for $\pi/2$-BPSK, $\pi/2$-ASK, MSK and OQAM signals whereas it is only an approximated model for GMSK signals [52].

In this paper, we limit the analysis to pulse shaping filters $v(t)$ corresponding, for R, π/2-BPSK and π/2-ASK constellations, to normalized (with unit energy) square-root raised cosine filter for the symbol duration T, with a roll-off ω and a bandwidth $B = (1+\omega)/T$. For OQAM constellations, $v(t)$ is a square-root raised cosine filter but for the symbol duration $2T$. Other filters $v(t)$ will be considered in the companion paper [50] for MSK and GMSK constellations in particular.

A2) *Total Noise SO statistics:* The SO statistics of $\mathbf{n}(t)$ are characterized by the two correlation matrices $\mathbf{R}_n(t,\tau)$ and $\mathbf{C}_n(t,\tau)$, defined by $\mathbf{R}_n(t,\tau) \stackrel{\text{def}}{=} \mathrm{E}[\mathbf{n}(t+\tau/2)\mathbf{n}^H(t-\tau/2)]$ and $\mathbf{C}_n(t,\tau) \stackrel{\text{def}}{=} \mathrm{E}[\mathbf{n}(t+\tau/2)\mathbf{n}^T(t-\tau/2)]$. Using (1), it is easy to verify that $\mathbf{R}_n(t,\tau)$ and $\mathbf{C}_n(t,\tau)$ are periodic functions of t, whose periods are equal to T and T, respectively for R signals, and to T and $2T$, respectively for QR signals. Matrices $\mathbf{R}_n(t,\tau)$ and $\mathbf{C}_n(t,\tau)$ have then Fourier series expansions given by

$$\mathbf{R}_n(t,\tau) = \sum_{\alpha_i} \mathbf{R}_n^{\alpha_i}(\tau) e^{j2\pi\alpha_i t} \quad (2)$$

$$\mathbf{C}_n(t,\tau) = \sum_{\beta_i} \mathbf{C}_n^{\beta_i}(\tau) e^{j2\pi\beta_i t}. \quad (3)$$

Here, α_i and β_i are the so-called non-conjugate and conjugate SO cyclic frequencies of $\mathbf{n}(t)$, such that $\alpha_i = i/T$ $(i \in \mathbb{Z})$ for both R and QR signals, whereas $\beta_i = i/T$ and $\beta_i = (2i+1)/2T$ $(i \in \mathbb{Z})$ for R and QR signals, respectively [54]–[56], $\mathbf{R}_n^{\alpha_i}(\tau)$ and $\mathbf{C}_n^{\beta_i}(\tau)$ are the first and second cyclic correlation matrices of $\mathbf{n}(t)$ for the cyclic frequencies α_i and β_i and the delay τ, defined by

$$\mathbf{R}_n^{\alpha_i}(\tau) \stackrel{\text{def}}{=} < \mathbf{R}_n(t,\tau) e^{-j2\pi\alpha_i t} > \quad (4)$$

$$\mathbf{C}_n^{\beta_i}(\tau) \stackrel{\text{def}}{=} < \mathbf{C}_n(t,\tau) e^{-j2\pi\beta_i t} >, \quad (5)$$

where $< . >$ is the temporal mean operation in t over an infinite observation duration. The Fourier transforms $\mathbf{R}_n^{\alpha_i}(f)$ and $\mathbf{C}_n^{\beta_i}(f)$, of $\mathbf{R}_n^{\alpha_i}(\tau)$ and $\mathbf{C}_n^{\beta_i}(\tau)$, respectively, are called the first and second cyclospectrum of $\mathbf{n}(t)$ for the cyclic frequencies α_i and β_i, respectively.

B. Extended models for standard or two-input WL processing

For both R and QR signals, a conventional linear processing of $\mathbf{x}(t)$ only exploits the information contained at the zero non-conjugate $(\alpha = 0)$ SO cyclic frequency of $\mathbf{x}(t)$, through the exploitation of the temporal mean of the first correlation matrix, $\mathbf{R}_x(t,\tau) \stackrel{\text{def}}{=} \mathrm{E}[\mathbf{x}(t+\tau/2)\mathbf{x}^H(t-\tau/2)]$, of $\mathbf{x}(t)$.

For R signals, a standard or two-input WL processing of $\mathbf{x}(t)$, only exploits the information contained at the zero non-conjugate and conjugate $(\alpha, \beta) = (0,0)$ SO cyclic frequencies of $\mathbf{x}(t)$ through the exploitation of the temporal mean of the first correlation matrix, $\mathbf{R}_{\tilde{x}}(t,\tau) \stackrel{\text{def}}{=} \mathrm{E}[\widetilde{\mathbf{x}}(t+\tau/2)\widetilde{\mathbf{x}}^H(t-\tau/2)]$, of the extended, or two-input model $\widetilde{\mathbf{x}}(t) \stackrel{\text{def}}{=} [\mathbf{x}^T(t), \mathbf{x}^H(t)]^T$, defined by

$$\widetilde{\mathbf{x}}(t) = \sum_{\ell} \widetilde{\mathbf{G}}(t-\ell T)\mathbf{b}_\ell + \widetilde{\boldsymbol{\epsilon}}(t) = \sum_{\ell} b_\ell \widetilde{\mathbf{g}}(t-\ell T) + \widetilde{\mathbf{n}}(t), \quad (6)$$

where $\widetilde{\boldsymbol{\epsilon}}(t) \stackrel{\text{def}}{=} [\boldsymbol{\epsilon}^T(t), \boldsymbol{\epsilon}^H(t)]^T$, $\widetilde{\mathbf{n}}(t) \stackrel{\text{def}}{=} [\mathbf{n}^T(t), \mathbf{n}^H(t)]^T$, $\widetilde{\mathbf{G}}(t) \stackrel{\text{def}}{=} [\widetilde{\mathbf{g}}(t), \widetilde{\mathbf{g}}_1(t), .., \widetilde{\mathbf{g}}_P(t)]$, $\widetilde{\mathbf{g}}(t) \stackrel{\text{def}}{=} [\mathbf{g}^T(t), \mathbf{g}^H(t)]^T$, $\widetilde{\mathbf{g}}_p(t) \stackrel{\text{def}}{=} [\mathbf{g}_p^T(t), \mathbf{g}_p^H(t)]^T$, $1 \le p \le P$, and $\mathbf{b}_\ell \stackrel{\text{def}}{=} [b_\ell, b_{1,\ell}, ...b_{P,\ell}]^T$.

For QR signals, as no information is contained at $\beta = 0$, a derotation preprocessing of the data is required before standard WL filtering. Using (1) for QR signals, the derotated observation vector can be written as

$$\begin{aligned}\mathbf{x}_d(t) &\stackrel{\text{def}}{=} j^{-t/T}\mathbf{x}(t) = \sum_{\ell}\mathbf{G}_d(t-\ell T)\mathbf{b}_\ell + \boldsymbol{\epsilon}_d(t) \\ &= \sum_{\ell} b_\ell \mathbf{g}_d(t-\ell T) + \mathbf{n}_d(t), \quad (7)\end{aligned}$$

where $\boldsymbol{\epsilon}_d(t) \stackrel{\text{def}}{=} j^{-t/T}\boldsymbol{\epsilon}(t)$, $\mathbf{n}_d(t) \stackrel{\text{def}}{=} j^{-t/T}\mathbf{n}(t)$, $\mathbf{G}_d(t) \stackrel{\text{def}}{=} [\mathbf{g}_d(t), \mathbf{g}_{1,d}(t), .., \mathbf{g}_{P,d}(t)] = v_d(t) \otimes \mathbf{H}_d(t)$, $\mathbf{g}_d(t) \stackrel{\text{def}}{=}$

$j^{-t/T}\mathbf{g}(t)$, $\mathbf{g}_{p,d}(t) \stackrel{\text{def}}{=} j^{-t/T}\mathbf{g}_p(t)$, $v_d(t) \stackrel{\text{def}}{=} j^{-t/T}v(t)$, $\mathbf{H}_d(t) \stackrel{\text{def}}{=} [\mathbf{h}_d(t), \mathbf{h}_{1,d}(t), .., \mathbf{h}_{P,d}(t)]$, $\mathbf{h}_d(t) \stackrel{\text{def}}{=} j^{-t/T}\mathbf{h}(t)$ and $\mathbf{h}_{p,d}(t) \stackrel{\text{def}}{=} j^{-t/T}\mathbf{h}_p(t)$. Note that we may also define alternatively $\mathbf{x}_d(t)$ by $\mathbf{x}_d(t) \stackrel{\text{def}}{=} j^{t/T}\mathbf{x}(t)$. Expression (7) shows that the derotation operation makes a QR signal looks like a R signal, with a non-zero information at the zero conjugate SO cyclic frequency. Indeed, it is easy to verify that $\mathbf{x}_d(t)$ has non-conjugate, $\alpha_{d,i}$ and conjugate, $\beta_{d,i}$, SO cyclic frequencies such that $\alpha_{d,i} = \alpha_i = i/T$ and $\beta_{d,i} = \beta_i - 1/2T = i/T$, which proves the presence of information at $\beta_{d,0} = 0$. Thus standard WL processing of QR signals, exploits the information contained at $(\alpha_{d,0}, \beta_{d,0}) = (0, 0)$ through the exploitation of the temporal mean of the first correlation matrix, $\mathbf{R}_{\widetilde{x}_d}(t,\tau) \stackrel{\text{def}}{=} \mathrm{E}[\widetilde{\mathbf{x}}_d(t+\tau/2)\widetilde{\mathbf{x}}_d^H(t-\tau/2)]$, of the extended, or two-input, derotated model $\widetilde{\mathbf{x}}_d(t) \stackrel{\text{def}}{=} [\mathbf{x}_d^T(t), \mathbf{x}_d^H(t)]^T$, defined by

$$\widetilde{\mathbf{x}}_d(t) = \sum_\ell \widetilde{\mathbf{G}}_d(t-\ell T)\mathbf{b}_\ell + \widetilde{\boldsymbol{\epsilon}}_d(t) = \sum_\ell b_\ell \widetilde{\mathbf{g}}_d(t-\ell T) + \widetilde{\mathbf{n}}_d(t), \tag{8}$$

where $\widetilde{\boldsymbol{\epsilon}}_d(t) \stackrel{\text{def}}{=} [\boldsymbol{\epsilon}_d^T(t), \boldsymbol{\epsilon}_d^H(t)]^T$, $\widetilde{\mathbf{n}}_d(t) \stackrel{\text{def}}{=} [\mathbf{n}_d^T(t), \mathbf{n}_d^H(t)]^T$, $\widetilde{\mathbf{G}}_d(t) \stackrel{\text{def}}{=} [\widetilde{\mathbf{g}}_d(t), \widetilde{\mathbf{g}}_{1,d}(t), .., \widetilde{\mathbf{g}}_{P,d}(t)]$, $\widetilde{\mathbf{g}}_d(t) \stackrel{\text{def}}{=} [\mathbf{g}_d^T(t), \mathbf{g}_d^H(t)]^T$ and $\widetilde{\mathbf{g}}_{p,d}(t) \stackrel{\text{def}}{=} [\mathbf{g}_{p,d}^T(t), \mathbf{g}_{p,d}^H(t)]^T$, $1 \le p \le P$.

C. M-input generic model for L and standard WL processing

In the following, we consider L and WL receivers as one and two-input receivers respectively. Then, for the M-input MMSE receivers ($M = 1, 2$), we denote by $\mathbf{x}_M(t)$ the generic observation vector. For linear receivers ($M = 1$), $\mathbf{x}_M(t)$ reduces to $\mathbf{x}(t)$ for R signals and to $\mathbf{x}_d(t)$ for QR signals. For standard WL receivers ($M = 2$), $\mathbf{x}_M(t)$ corresponds to $\widetilde{\mathbf{x}}(t)$ for R signals and to $\widetilde{\mathbf{x}}_d(t)$ for QR signals. We then deduce from (1), (6), (7) and (8), that $\mathbf{x}_M(t)$ always takes the form

$$\begin{aligned}\mathbf{x}_M(t) &= \sum_\ell b_\ell \mathbf{g}_M(t-\ell T) + \sum_{1\le p\le P}\sum_\ell b_{p,\ell}\mathbf{g}_{p,M}(t-\ell T) + \boldsymbol{\epsilon}_M(t) \\ &= \sum_\ell \mathbf{G}_M(t-\ell T)\mathbf{b}_\ell + \boldsymbol{\epsilon}_M(t) \\ &\stackrel{\text{def}}{=} \sum_\ell b_\ell \mathbf{g}_M(t-\ell T) + \mathbf{n}_M(t). \end{aligned} \tag{9}$$

Here, $\mathbf{g}_M(t)$, $\mathbf{g}_{p,M}(t)$, $\boldsymbol{\epsilon}_M(t)$ and $\mathbf{n}_M(t)$ are defined in a similar way as $\mathbf{x}_M(t)$, where $\mathbf{x}(t)$ is replaced by $\mathbf{g}(t)$, $\mathbf{g}_p(t)$, $\boldsymbol{\epsilon}(t)$ and $\mathbf{n}(t)$, respectively, whereas $\mathbf{G}_1(f) = \mathbf{G}(f)$ for R signals and $\mathbf{G}_1(f) = \mathbf{G}_d(f)$ for QR signals, $\mathbf{G}_2(f) = \widetilde{\mathbf{G}}(f)$ for R signals and $\mathbf{G}_2(f) = \widetilde{\mathbf{G}}_d(f)$ for QR signals.

III. Linear and WL MMSE receivers

In this section, we compute, for R and QR signals, L and two-input WL MMSE receivers, both without and with a structure constraint, fully exploiting (in the two cases) or not (without any structure constraint) the MUI waveform knowledge.

A. L and WL MMSE receivers without any structure constraint

A1) *Presentation:* In order to simplify their implementation, most of the L and WL MMSE receivers of the literature are computed at the symbol rate after a matched filtering operation to the pulse shaping filter. They have thus a particular structure constraint, which is shown in this paper to be generally sub-optimal at least for frequency selective channels for R and QR signals, and which prevents from exploiting the SO cyclostationary property of the MUI. To evaluate the impact on performance of this generally sub-optimal structure constraint, it is necessary to compute the L and WL MMSE receivers without any structure constraint, noting that the latter may fully exploit or not the SO cyclostationary property of the MUI. A generic M-input MMSE receiver having no structure constraint corresponds to a continuous-time (CT) receiver, $\mathbf{w}_M^*(-t)$ of dimension $N \times 1$ (for $M = 1$) and $2N \times 1$ (for $M = 2$), whose output, $y_M(t) = \mathbf{w}_M^H(-t) \otimes \mathbf{x}_M(t)$, minimizes, at each time sample nT, the MSE criterion, $\mathrm{MSE} = \mathrm{E}(|b_n - y_M(nT)|^2)$. This MSE criterion minimization may fully exploit or not the waveform knowledge of MUI, and thus, implicitly, their SO cyclostationary property.

A2) *Optimal MMSE receivers or MMSE receivers fully exploiting the MUI waveform knowledge:* Fully exploiting the MUI waveform knowledge in the M-input MMSE receiver computation consists to take into account the explicit MUI form appearing in model (1), which implicitly consists to take into account the SO cyclostationarity of the MUI, for $M = 1, 2$, in addition to their SO non-circularity, for $M = 2$. Once the SO cyclostationarity of MUI is fully exploited, estimating the SOI symbols only or jointly with the MUI symbols gives rise to two equivalent approaches[1] for the SOI symbols estimation, as explained in Appendix A. In other words, we deduce from (9) that the filter $\mathbf{w}_M^*(-t)$ minimizing the MSE criterion corresponds to the first column of the matrix $\mathbf{W}_M^*(-t)$, of dimension $N \times (P + 1)$ for $M = 1$ and $2N \times (P + 1)$ for $M = 2$, minimizing the joint MSE criterion, $\mathrm{JMSE} = \mathrm{E}(\|\mathbf{b}_n - \mathbf{y}_M(nT)\|^2)$. In the latter criterion, $\mathbf{b}_n$ has been defined in Section II-B, whereas $\mathbf{y}_M(t)$ is defined by $\mathbf{y}_M(t) = \mathbf{W}_M^H(-t) \otimes \mathbf{x}_M(t)$. Denoting by $\mathbf{w}_{M_0}^*(-t)$, the M-input receiver which minimizes the MSE criterion (i.e., the optimal M-input MMSE receiver), it is proved in Appendix A that the frequency response, $\mathbf{w}_{M_0}^*(f)$, of this receiver, denoted by (o) in the following,

[1] Note that the approach consisting to jointly estimate the SOI and MUI symbols involves that the additive noise is SO stationary. Whereas, considering the estimation of the SOI symbols only involves that the total noise is SO cyclostationary, which implies a more complicated derivation of (10).

is such that

$$\begin{aligned}\mathbf{w}_{M_o}(f) &= \mathbf{G}_M(f)[(N_0/\pi_b)\mathbf{I}_{P+1} \\ &+ 1/T\sum_{\ell}\mathbf{G}_M^H(f-\ell/T)\mathbf{G}_M(f-\ell/T)]^{-1}\mathbf{f} \\ &\stackrel{\text{def}}{=} \mathbf{G}_M(f)\mathbf{C}_{M_o}^d(f)\mathbf{f} \stackrel{\text{def}}{=} \mathbf{G}_M(f)\mathbf{c}_{M_o}^d(f). \quad (10)\end{aligned}$$

Here $\pi_b \stackrel{\text{def}}{=} \mathrm{E}(b_k^2)$, N_0 is the power spectral density of each component of the noise vector $\boldsymbol{\epsilon}(t)$, $\mathbf{f}$ is the $(P+1)\times 1$ vector defined by $\mathbf{f} = [1, 0, ..., 0]^T$, $\mathbf{C}_{M_0}^d(f)$ is the $(P+1)\times(P+1)$ inverse matrix appearing in (10), which is periodic of period $1/T$, whereas $\mathbf{c}_{M_0}^d(f) \stackrel{\text{def}}{=} \mathbf{C}_{M_0}^d(f)\mathbf{f}$ is a $(P+1)\times 1$ vector. The output, at time kT, of the associated receiver is given by

$$\begin{aligned}y_{M_0}(k) &= \int \mathbf{w}_{M_0}^H(f)\mathbf{x}_M(f)e^{j2\pi fkT}df \\ &= \int {\mathbf{c}_{M_o}^d}^H(f)\mathbf{G}_M^H(f)\mathbf{x}_M(f)e^{j2\pi fkT}df, \quad (11)\end{aligned}$$

To make $\mathbf{c}_{M_o}^d(f)$ more concrete, we compute its expression in the presence of $P = 1$ MUI, which gives in this case $\mathbf{c}_{M_o}^d(f) = [c_{M,1}^d(f), c_{M,2}^d(f)]^T$, where $c_{M,1}^d(f)$ and $c_{M,2}^d(f)$ are given by

$$c_{M,1}^d(f) = \frac{\pi_b(N_0 + \frac{\pi_b}{T}\sum_\ell \|\mathbf{g}_{1,M}(f-\frac{\ell}{T})\|^2)}{\left\{\begin{array}{l}(N_0+\frac{\pi_b}{T}\sum_\ell \|\mathbf{g}_M(f-\frac{\ell}{T})\|^2) \\ \qquad (N_0+\frac{\pi_b}{T}\sum_\ell \|\mathbf{g}_{1,M}(f-\frac{\ell}{T})\|^2) \\ -\frac{\pi_b^2}{T^2}|\sum_\ell \mathbf{g}_M^H(f-\frac{\ell}{T})\mathbf{g}_{1,M}(f-\frac{\ell}{T})|^2\end{array}\right.} \quad (12)$$

$$c_{M,2}^d(f) = \frac{-\frac{\pi_b^2}{T}\sum_\ell \mathbf{g}_{1,M}^H(f-\frac{\ell}{T})\mathbf{g}_M(f-\frac{\ell}{T})}{\left\{\begin{array}{l}(N_0+\frac{\pi_b}{T}\sum_\ell \|\mathbf{g}_M(f-\frac{\ell}{T})\|^2) \\ \qquad (N_0+\frac{\pi_b}{T}\sum_\ell \|\mathbf{g}_{1,M}(f-\frac{\ell}{T})\|^2) \\ -\frac{\pi_b^2}{T^2}|\sum_\ell \mathbf{g}_M^H(f-\frac{\ell}{T})\mathbf{g}_{1,M}(f-\frac{\ell}{T})|^2\end{array}\right.} \quad (13)$$

where $\mathbf{G}_M(f) \stackrel{\text{def}}{=} [\mathbf{g}_{M,}(f), \mathbf{g}_{1,M}(f)]$. Expressions (10) and (11) show that, for both R and QR signals, optimal L and WL MMSE receivers are composed of three operations, as depicted in Fig.1 The first one, $\mathbf{G}_M^H(f)$, implements a set of $P+1$ CT matched filtering operation to the global channels of SOI and MUI. The second one is a sampling, to the symbol rate, of each of these matched filter outputs. The third one, ${\mathbf{c}_{M_0}^d}^H(f)$, implements a set of $P+1$ discrete-time (TD) or digital filtering operations, applied to the previous $P+1$ sampled outputs, which performs the SOI channel equalization jointly with the noise plus MUI minimization. Note that the implementation of the receivers (10) requires the a priori knowledge or estimation of N_0 and $\mathbf{G}(t)$, and then of $\mathbf{H}(t)$, i.e., of the impulse response of both the SOI and MUI channel vectors, which may be cumbersome for a practical implementation.

A3) *Sub-optimal MMSE receivers falsely assuming SO stationary MUI:* In order to throw off the MUI channel estimation, one may prefer not to fully take into account the MUI waveform knowledge, and thus their cyclostationarity, by estimating the SOI symbols only, assuming that the MUI

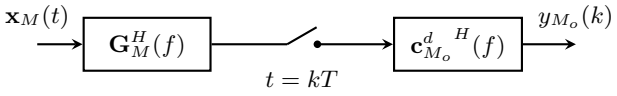

Fig. 1. Structure of the optimal MMSE receiver

are falsely SO stationary. Denoting by $\mathbf{w}_{M_s}^*(-t)$, the M-input receiver which minimizes the MSE criterion, assuming that the MUI, and thus the total noise $\mathbf{n}(t)$, is falsely SO stationary, it is proved in Appendix B that the frequency response, $\mathbf{w}_{M_s}^*(f)$, of this receiver, denoted by (s) in the following, is such that

$$\begin{aligned}\mathbf{w}_{M_s}(f) &= \Big\{(1/\pi_b) + (1/T)\sum_\ell \mathbf{g}_M^H(f-\ell/T) \\ &[\mathbf{R}_{n,M}^0(f-\ell/T)]^{-1}\mathbf{g}_M(f-\ell/T)\Big\}^{-1}[\mathbf{R}_{n_M}^0(f)]^{-1}\mathbf{g}_M(f) \\ &\stackrel{\text{def}}{=} c_{M_s}^d(f)[\mathbf{R}_{n_M}^0(f)]^{-1}\mathbf{g}_M(f). \quad (14)\end{aligned}$$

Here, $c_{M_s}^d(f)$ is the inverse scalar term appearing in (14), which is periodic of period $1/T$, $\mathbf{g}_1(f) = \mathbf{g}(f)$ for R signals and $\mathbf{g}_1(f) = \mathbf{g}_d(f)$ for QR signals, $\mathbf{g}_2(f) = \widetilde{\mathbf{g}}(f)$ for R signals and $\mathbf{g}_2(f) = \widetilde{\mathbf{g}}_d(f)$ for QR signals, $\mathbf{R}_{n_M}^0(f)$ defined as the Fourier transform of $\mathbf{R}_{n_M}^0(\tau) \stackrel{\text{def}}{=} < \mathrm{E}[\mathbf{n}_M(t+\tau/2)\mathbf{n}_M^H(t-\tau/2)] >$ corresponds to the power spectral density matrix of $\mathbf{n}_M(t)$. Using (1), it is easy to verify that $\mathbf{R}_{n_M}^0(f)$ is given by

$$\begin{aligned}\mathbf{R}_{n_M}^0(f) &= \frac{\pi_b}{T}\sum_{1\le p\le P}\mathbf{g}_{p,M}(f)\mathbf{g}_{p,M}^H(f) + N_0\mathbf{I}_{NM} \\ &= \mathbf{R}_{x_M}^0(f) - \frac{\pi_b}{T}\mathbf{g}_M(f)\mathbf{g}_M^H(f), \quad (15)\end{aligned}$$

where $\mathbf{g}_{p,M}(f)$ is defined in a similar way as $\mathbf{g}_M(f)$ but where $\mathbf{g}(f)$ is replaced by $\mathbf{g}_p(f)$ and where $\mathbf{R}_{x_M}^0(f)$ is the power spectral density matrix of $\mathbf{x}_M(t)$, defined in a similar way as $\mathbf{R}_{n_M}^0(f)$, with $\mathbf{x}_M(t)$ instead of $\mathbf{n}_M(t)$. The output, at time kT, of the associated receiver is given by

$$\begin{aligned}y_{M_s}(k) &= \int \mathbf{w}_{M_s}^H(f)\mathbf{x}_M(f)e^{j2\pi fkT}df \\ &= \int c_{M_s}^d(f)\mathbf{g}_M^H(f)[\mathbf{R}_{n_M}^0(f)]^{-1}\mathbf{x}_M(f)e^{j2\pi fkT}df \quad (16)\end{aligned}$$

Expressions (14) and (16) show that, for both R and QR signals, sub-optimal L and WL MMSE receivers without any structure constraint falsely assuming SO stationary MUI, are composed of three operations, as depicted in Fig.2. The first one, $\mathbf{g}_M^H(f)[\mathbf{R}_{n_M}^0(f)]^{-1}$, implements a CT M-input spatio-temporal or spatio-frequential pseudo-matched filter to the global channel of the SOI in a spatially and temporally colored total noise. The second operation is a sampling, to the symbol rate, of this pseudo-matched filter output. The third one, $c_{M_s}^d(f)$, implements a scalar digital filtering operation, corresponding to a pseudo-MMSE equalizer of the SOI channel at the output of the pseudo-matched filter.

Note that the implementation of the receivers (14) requires the a priori knowledge or estimation of $\mathbf{R}_n^0(f)$ and $\mathbf{g}(t)$, and then of $\mathbf{h}(t)$, i.e., of the impulse response of the SOI channel vector only, discarding the need to estimate the MUI channel vectors, which may be advantageous for a practical implementation.

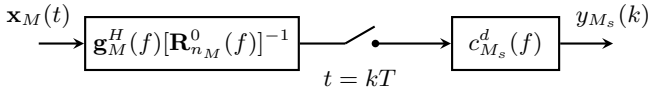

Fig. 2. Structure of the sub-optimal MMSE receiver falsely assuming stationary MUI

B. L and WL MMSE receivers with a particular structure constraint

B1) *Presentation:* Contrary to L and WL MMSE receivers (10) and (14), which have no structure constraint, most of L and WL MMSE receivers of the literature are implemented at the symbol rate, after a matched filtering operation to the pulse shaping filter, and have thus a particular and generally sub-optimal structure constraint in most cases. It is then important to consider and to compute these constrained receivers in order to compare their performance to those of receivers (o) (10) and (s) (14). Denoting by $\mathbf{x}_v(t) \stackrel{\text{def}}{=} v^*(-t) \otimes \mathbf{x}(t)$, the observation vector after matched filtering operation to the pulse-shaping filter, we deduce from (1) and (9) that, after the sampling operation at the symbol rate, the M-input observation vector becomes,

$$\begin{aligned}\mathbf{x}_{v,M}(nT) &= \sum_\ell b_\ell \mathbf{g}_{v,M}((n-\ell)T) \\ &+ \sum_{1\le p\le P}\sum_\ell b_{p,\ell}\mathbf{g}_{p_{v,M}}((n-\ell)T) + \boldsymbol{\epsilon}_{v,M}(nT) \\ &= \sum_\ell \mathbf{G}_{v,M}((n-\ell)T)\mathbf{b}_\ell + \boldsymbol{\epsilon}_{v,M}(nT) \\ &\stackrel{\text{def}}{=} \sum_\ell b_\ell \mathbf{g}_{v,M}((n-\ell)T) + \mathbf{n}_{v,M}(nT). \quad (17)\end{aligned}$$

Here, $\mathbf{x}_{v,M}(t)$, $\mathbf{g}_{v,M}(t)$, $\mathbf{g}_{p_{v,M}}(t)$, $\boldsymbol{\epsilon}_{v,M}(t)$ and $\mathbf{n}_{v,M}(t)$ are defined in a similar way as $\mathbf{x}_M(t)$, where $\mathbf{x}(t)$ is replaced by $\mathbf{x}_v(t)$, $\mathbf{g}_v(t)$, $\mathbf{g}_{p_v}(t)$, $\boldsymbol{\epsilon}_v(t)$ and $\mathbf{n}_v(t)$ respectively, with $\mathbf{a}_v(t) \stackrel{\text{def}}{=} v^*(-t) \otimes \mathbf{a}(t)$, whereas $\mathbf{G}_{v,M}(t)$ is defined in a similar way as $\mathbf{G}_M(t)$ where $\mathbf{g}_v(t)$ and $\mathbf{g}_{p_v}(t)$ replace $\mathbf{g}(t)$ and $\mathbf{g}_p(t)$, respectively. Denoting by ${\mathbf{w}^d_{M_{sc}}}^*(-kT)$, the M-input discrete time (DT) receiver whose output at time nT, $y_M(nT) = \sum_k {\mathbf{w}^d_{M_{sc}}}^H(-kT)\mathbf{x}_{v,M}((n-k)T))$, minimizes the MSE, it is proved in Appendix C that the frequency response, ${\mathbf{w}^d_{M_{sc}}}^*(f)$, of this receiver, denoted by (sc) in the following, is such that

$$\begin{aligned}\mathbf{w}^d_{M_{sc}}(f) &= \pi_b[\mathbf{R}^d_{x_{v,M}}(f)]^{-1}\mathbf{g}^d_{v,M}(f) \\ &= \Big[1/\pi_b + {\mathbf{g}^d_{v,M}}^H(f)[\mathbf{R}^d_{n_{v,M}}(f)]^{-1}\mathbf{g}^d_{v,M}(f)\Big]^{-1} \\ &\qquad [\mathbf{R}^d_{n_{v,M}}(f)]^{-1}\mathbf{g}^d_{v,M}(f) \\ &\stackrel{\text{def}}{=} c^d_{M_{sc}}(f)[\mathbf{R}^d_{n_{v,M}}(f)]^{-1}\mathbf{g}^d_{v,M}(f), \quad (18)\end{aligned}$$

if $v(f)$ does not vanish in $[-1/2T, +1/2T]$. Otherwise $\mathbf{w}^d_{M_{sc}}(f) = \mathbf{0}$ for the frequencies f which are outside the support of $\mathbf{g}^d_{v,M}(f)$, i.e., such that $\mathbf{x}^d_{v,M}(f) = \mathbf{0}$, where $\mathbf{x}^d_{v,M}(f)$ is the Fourier transform of $\mathbf{x}_{v,M}(nT)$. Here, $c^d_{M_{sc}}(f)$ and $\mathbf{g}^d_{v,M}(f)$, both periodic of period $1/T$, are the inverse scalar term appearing in (18) and the frequency response of the DT SOI channel vector $\mathbf{g}_{v,M}(kT)$, respectively, such that

$$\mathbf{g}^d_{v,M}(f) = \sum_k \mathbf{g}_{v,M}(kT)e^{-j2\pi fkT} = \frac{1}{T}\sum_\ell \mathbf{g}_{v,M}(f - \frac{\ell}{T}). \quad (19)$$

Matrices $\mathbf{R}^d_{x_{v,M}}(f)$ and $\mathbf{R}^d_{n_{v,M}}(f)$ are the Fourier transforms of matrices $\mathbf{R}^d_{x_{v,M}}(kT) \stackrel{\text{def}}{=} \mathrm{E}[\mathbf{x}_{v,M}(nT)\mathbf{x}^H_{v,M}((n-k)T)]$ and $\mathbf{R}^d_{n_{v,M}}(kT) \stackrel{\text{def}}{=} \mathrm{E}[\mathbf{n}_{v,M}(nT)\mathbf{n}^H_{v,M}((n-k)T)]$, respectively, where the DT vectors $\mathbf{x}_{v,M}(nT)$ and $\mathbf{n}_{v,M}(nT)$ are SO stationary, defined by

$$\begin{aligned}\mathbf{R}^d_{x_{v,M}}(f) &= \sum_k \mathbf{R}^d_{x_{v,M}}(kT)e^{-j2\pi fkT} \\ &= \mathbf{R}^d_{n_{v,M}}(f) + \pi_b \mathbf{g}^d_{v,M}(f){\mathbf{g}^d_{v,M}}^H(f). \quad (20) \\ \mathbf{R}^d_{n_{v,M}}(f) &= \sum_k \mathbf{R}^d_{n_{v,M}}(kT)e^{-j2\pi fkT} \\ &= \sum_{p=1}^P \pi_b \mathbf{g}^d_{p_{v,M}}(f){\mathbf{g}^d_{p_{v,M}}}^H(f) + \mathbf{R}^d_{\epsilon_{v,M}}(f) \quad (21)\end{aligned}$$

Here $\mathbf{g}^d_{p_{v,M}}(f)$ is defined similarly as $\mathbf{g}^d_{v,M}(f)$, where $\mathbf{g}_{v,M}(kT)$ is replaced by $\mathbf{g}_{p_{v,M}}(kT)$, and $\mathbf{R}^d_{\epsilon_{v,M}}(f)$ is the Fourier Transform of $\mathbf{R}^d_{\epsilon_{v,M}}(kT) \stackrel{\text{def}}{=} \mathrm{E}[\boldsymbol{\epsilon}_{v,M}(nT)\boldsymbol{\epsilon}^H_{v,M}((n-k)T)]$, defined by

$$\mathbf{R}^d_{\epsilon_{v,M}}(f) = \sum_k \mathbf{R}^d_{\epsilon_{v,M}}(kT)e^{-j2\pi fkT} = \frac{1}{T}\sum_\ell \mathbf{R}_{\epsilon_{v,M}}(f - \frac{\ell}{T}), \quad (22)$$

where $\mathbf{R}_{\epsilon_{v,M}}(f)$ is the Fourier transform of $\mathbf{R}_{\epsilon_{v,M}}(\tau) \stackrel{\text{def}}{=} \mathrm{E}[\boldsymbol{\epsilon}_{v,M}(t+\tau/2)\boldsymbol{\epsilon}^H_{v,M}(t-\tau/2)]$, since $\boldsymbol{\epsilon}_{v,M}(t)$ is SO stationary. Note that the second equality of (18) comes from the application of the Woodbury Identity to $[\mathbf{R}^d_{x_{v,M}}(f)]^{-1}$, using (20). The output, at time kT, of the associated receiver is given by

$$\begin{aligned}y_{M_{sc}}(k) &= T\int_\Delta {\mathbf{w}^d_{M_{sc}}}^H(f)\mathbf{x}^d_{v,M}(f)e^{j2\pi fkT}df \\ &= \int {\mathbf{w}^d_{M_{sc}}}^H(f)\mathbf{x}_{v,M}(f)e^{j2\pi fkT}df \\ &= T\int_\Delta c^d_{M_{sc}}(f){\mathbf{g}^d_{v,M}}^H(f)[\mathbf{R}^d_{n_{v,M}}(f)]^{-1}\mathbf{x}^d_{v,M}(f)e^{j2\pi fkT}df \\ &= \int c^d_{M_{sc}}(f){\mathbf{g}^d_{v,M}}^H(f)[\mathbf{R}^d_{n_{v,M}}(f)]^{-1}\mathbf{x}_{v,M}(f)e^{j2\pi fkT}df \quad (23)\end{aligned}$$

where $\Delta \stackrel{\text{def}}{=} [-1/2T, 1/2T]$. Note that when $v(f)$ vanishes in Δ, the integration appearing in (23) is over the frequency support of $\mathbf{x}^d_{v,M}(f)$ or $\mathbf{x}_{v,M}(f)$. Expressions (18) and (23) show that, for both R and QR signals, sub-optimal L and WL MMSE receivers with the structure constraint of the

literature, are composed of two operations, as depicted in Fig.3. The first one, ${\mathbf{g}^d_{v,M}}^H(f)[\mathbf{R}^d_{n_{v,M}}(f)]^{-1}$, implements a DT M-input spatio-temporal or spatio-frequential matched filter to the global channel of the SOI in a spatially and temporally colored total noise, which is stationary in this case. The second one, $c^d_{M_{sc}}(f)$, implements a scalar digital filtering operation, corresponding to an MMSE equalizer of the SOI channel at the output of the matched filter. Note that the implementation of the receivers (18) requires the a priori knowledge or estimation of $\mathbf{R}^d_{x_{v,M}}(f)$ and $\mathbf{g}^d_{v,M}(f)$ and then of $\mathbf{h}(kT)$, i.e,. of the DT impulse response of the SOI channel vector only. Comparing (18) to (14), we find that $\mathbf{w}^d_{M_{sc}}(f)$ and $\mathbf{w}_{M_s}(f)$, both exploiting a true and false SO stationarity property of the MUI respectively, have very similar forms but where the matched filter to the SOI global channel in colored noise is CT in (14) and DT in (18), at the symbol rate.

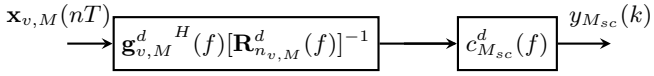

Fig. 3. Structure of the sub-optimal MMSE receiver with a structure constraint

B2) *Equivalence with the MMSE receivers jointly estimating the SOI and MUI symbols:* While receivers (18) have a similar form as receivers (14), since the MUI become SO stationary with the considered structure constraint, they should also have a form similar to (10), since the structure constraint also allows us to fully exploit the MUI waveform knowledge in (18). Denoting by $\mathbf{G}^d_{v,M}(f)$, the Fourier transform of $\mathbf{G}_{v,M}(kT)$, it is proved in Appendix C that (18) can also be written as

$$\begin{aligned}\mathbf{w}^d_{M_{sc}}(f) &= \pi_b[\mathbf{R}^d_{x_{v,M}}(f)]^{-1}\mathbf{G}^d_{v,M}(f)\mathbf{f}\\ &= [\mathbf{R}^d_{\epsilon_{v,M}}(f)]^{-1}\mathbf{G}^d_{v,M}(f)\{(1/\pi_b)\mathbf{I}_{P+1}\\ &+{\mathbf{G}^d_{v,M}}^H(f)[\mathbf{R}^d_{\epsilon_{v,M}}(f)]^{-1}\mathbf{G}^d_{v,M}(f)\}^{-1}\mathbf{f}, \quad (24)\end{aligned}$$

where $\mathbf{f}$ has been defined in (10). Expression (24) is similar to (10), except for two points. The first one is that the background noise is colored in (17) but not in (9), hence the presence of $\mathbf{R}^d_{\epsilon_{v,M}}(f)$ matrix in (24) instead of $N_0\mathbf{I}_{NM}$ matrix in (10). The second one is that the set of DT matched filters to the global channels of SOI and MUI in colored background noise, $[\mathbf{R}^d_{x_{v,M}}(f)]^{-1}\mathbf{G}^d_{v,M}(f)$, replaces the set of CT matched filters to the global channels of SOI and MUI in white background noise, $\mathbf{G}_M(f)$. We then deduce from this result that the DT filter, ${\mathbf{w}^d_{M_{sc}}}^*(-kT)$, whose output at time nT, $y_M(nT) = \sum_k {\mathbf{w}^d_{M_{sc}}}^H(-kT)\mathbf{x}_{v,M}((n-k)T))$, minimizes the MSE, also corresponds to the first column of the DT matrix, ${\mathbf{W}^d_{M_{sc}}}^*(-kT)$, whose output vector at time nT, $\mathbf{y}_M(nT) = \sum_k {\mathbf{W}^d_{M_{sc}}}^H(-kT)\mathbf{x}_{v,M}((n-k)T))$, minimizes the joint MSE, JMSE = $\mathrm{E}(\|\mathbf{b}_n - \mathbf{y}_M(nT)\|^2)$.

C. Particular case of an absence of MUI

In the absence of MUI, the total noise is SO stationary and thus the sub-optimal MMSE receivers falsely assuming SO stationary MUI are the optimal MMSE receivers. So $\mathbf{G}_M(f)$, $\mathbf{R}_{n,M}(f)$ and $\mathbf{R}^d_{n_{v,M}}(f)$ reduce to $\mathbf{g}_M(f)$, $\mathbf{R}_{\epsilon,M}(f) = N_0\mathbf{I}_{NM}$ and $\mathbf{R}^d_{\epsilon_{v,M}}(f)$, respectively, and we deduce from (10), (14) and (18) that:

$$\begin{aligned}\mathbf{w}_{M_o}(f) &= \mathbf{w}_{M_s}(f) =\\ &\{(N_0/\pi_b) + (1/T)\sum_\ell \|\mathbf{g}_M(f-\ell/T)\|^2\}^{-1}\mathbf{g}_M(f) \quad (25)\end{aligned}$$

$$\begin{aligned}\mathbf{w}^d_{M_{sc}}(f) = \{1/\pi_b + {\mathbf{g}^d_{v,M}}^H(f)[\mathbf{R}^d_{\epsilon_{v,M}}(f)]^{-1}\mathbf{g}^d_{v,M}(f)\}^{-1}\\ [\mathbf{R}^d_{\epsilon_{v,M}}(f)]^{-1}\mathbf{g}^d_{v,M}(f). \quad (26)\end{aligned}$$

Inserting (25) in (11) and (26) in (23), it is straightforward to show that in the general case of a frequency selective SOI channel, $y_{M_{sc}}(k)$ and $y_{M_o}(k)$ are generally different, which shows the sub-optimality of L and WL MMSE receivers with the structure constraint, and thus of most of L and WL MMSE receivers of the literature. Nevertheless, a more detailed analysis of $y_{M_{sc}}(k)$ and $y_{M_o}(k)$ allows us to prove the equality of $y_{M_{sc}}(k)$, $y_{M_s}(k)$ and $y_{M_o}(k)$, and thus the optimality of (26), if one of the two following conditions is verified

(a) $\mathbf{h}(f) = \mathbf{h}$ (27)

(b) The bandwidth of $v(t)$ is included in Δ. (28)

Note that condition (b) is verified for OQAM constellations.

IV. SINR at the output of the linear an WL MMSE receivers

In this section, we first compute the general expressions of the SINR at the output of the previous L and WL MMSE receivers before decision and then we compare these SINR, for R and QR signals and for some particular propagation channels, when the total noise is composed of background noise plus zero or one MUI.

A. Generic output of the linear and WL MMSE receivers before decision

We deduce from (11), (16) and (23) that the generic output of the L and WL receivers considered in this paper can be written as

$$y_{M_g}(k) = \int \mathbf{w}^H_{M_g}(f)\mathbf{x}_{M_g}(f)e^{j2\pi fkT}df \quad (29)$$

where it is easy to verify from (9) and (17) that

$$\mathbf{x}_{M_g}(f) = \sum_\ell b_l e^{-j2\pi f\ell T}\mathbf{g}_{M_g}(f) + \mathbf{n}_{M_g}(f). \quad (30)$$

Note that $(y_{M_g}(k), \mathbf{w}_{M_g}(f), \mathbf{x}_{M_g}(f), \mathbf{g}_{M_g}(f), \mathbf{n}_{M_g}(f)) = (y_{M_o}(k), \mathbf{w}_{M_o}(f), \mathbf{x}_M(f), \mathbf{g}_M(f), \mathbf{n}_M(f))$,
$(y_{M_g}(k), \mathbf{w}_{M_g}(f), \mathbf{x}_{M_g}(f), \mathbf{g}_{M_g}(f), \mathbf{n}_{M_g}(f)) =$

$(y_{M_s}(k), \mathbf{w}_{M_s}(f), \mathbf{x}_M(f), \mathbf{g}_M(f), \mathbf{n}_M(f))$ and $(y_{M_g}(k), \mathbf{w}_{M_g}(f), \mathbf{x}_{M_g}(f), \mathbf{g}_{M_g}(f), \mathbf{n}_{M_g}(f)) = (y_{M_{sc}}(k), \mathbf{w}^d_{M_{sc}}(f), \mathbf{x}_{v_M}(f), \mathbf{g}_{v_M}(f), \mathbf{n}_{v_M}(f))$ for the receivers of Sections III-A2, III-A3, and III-B1, respectively. Inserting (30) into (29), we obtain:

$$\begin{aligned} y_{M_g}(k) &= b_k \int \mathbf{w}^H_{M_g}(f)\mathbf{g}_{M_g}(f)df \\ &+ \sum_{\ell \neq k} b_\ell \int \mathbf{w}^H_{M_g}(f)\mathbf{g}_{M_g}(f)e^{j2\pi f(k-\ell)T}df \\ &+ \int \mathbf{w}^H_{M_g}(f)\mathbf{n}_{M_g}(f)e^{j2\pi fkT}df \stackrel{\text{def}}{=} b_k u_{M_g} + e_{M_g}(k), \quad (31) \end{aligned}$$

where it is easy to verify that u_{M_g} is a real-valued quantity and where $e_{M_g}(k)$ is the contribution of the Intersymbol Interference (ISI), the MUI and the background noise in $y_{M_g}(k)$. As b_k is a real-valued symbol, it is well-known that, assuming a circular Gaussian $e_{M_g}(k)$, a conventional ML receiver whose input is (31), decides the symbols from the real-part of $y_{M_g}(k)$, given by

$$z_{M_g}(k) \stackrel{\text{def}}{=} \text{Re}(y_{M_g}(k)) = b_k u_{M_g} + \text{Re}(e_{M_g}(k)). \quad (32)$$

B. Generic SINR at the output of the linear and WL MMSE receivers before decision

The SER at the output of the generic receiver $\mathbf{w}^H_{M_g}(f)$ is directly linked to the SINR in $z_{M_g}(k)$, denoted by $\text{SINR}_{M_g}(k)$. Using the fact that the quantities $b_k u_{M_g}$ and $\text{Re}(e_{M_g}(k))$ are uncorrelated, we deduce that $\text{SINR}_{M_g}(k)$ can be written as

$$\begin{aligned} \text{SINR}_{M_g}(k) &= \frac{\pi_b u^2_{M_g}}{\text{E}[(\text{Re}(e_{M_g}(k)))^2]} \\ &= \frac{2\pi_b u^2_{M_g}}{\text{E}[|y^2_{M_g}(k)|] + \text{Re}(\text{E}[y^2_{M_g}(k)]) - 2\pi_b u^2_{M_g}}. \quad (33) \end{aligned}$$

In the presence of R or QR MUI, the CT output[2] $y_{M_g}(t)$ is SO cyclostationary, which implies that $\text{E}[|y^2_{M_g}(k)|]$ and $\text{E}[y^2_{M_g}(k)]$ have Fourier series expansions given by [48].

$$\text{E}[|y^2_{M_g}(k)|] = \sum_{\gamma_i} e^{j2\pi\gamma_i kT} \int r^{\gamma_i}_{y_{M_g}}(f)df \quad (34)$$

$$\text{E}[y^2_{M_g}(k)] = \sum_{\delta_i} e^{j2\pi\delta_i kT} \int c^{\delta_i}_{y_{M_g}}(f)df. \quad (35)$$

Here, the quantities γ_i and δ_i denote the non-conjugate and conjugate SO cyclic frequencies of $y_{M_g}(t)$, respectively, whereas $r^{\gamma_i}_{y_{M_g}}(f)$ and $c^{\delta_i}_{y_{M_g}}(f)$ are the Fourier transforms of the first, $r^{\gamma_i}_{y_{M_g}}(\tau)$, and second, $c^{\delta_i}_{y_{M_g}}(\tau)$, cyclic correlation functions of $y_{M_g}(t)$ for the delay τ and the cyclic frequencies γ_i and δ_i, respectively. Moreover, as $y_{M_g}(t)$ is the output of the TI filter $\mathbf{w}^H_{M_g}(f)$ whose input is $\mathbf{x}_{M_g}(t)$, we can write

$$r^{\gamma_i}_{y_{M_g}}(f) = \mathbf{w}^H_{M_g}(f+\gamma_i/2)\mathbf{R}^{\gamma_i}_{x_{M_g}}(f)\mathbf{w}_{M_g}(f-\gamma_i/2) \quad (36)$$

$$c^{\delta_i}_{y_{M_g}}(f) = \mathbf{w}^H_{M_g}(f+\delta_i/2)\mathbf{C}^{\delta_i}_{x_{M_g}}(f)\mathbf{w}^*_{M_g}(\delta_i/2-f), \quad (37)$$

where $\mathbf{R}^{\gamma_i}_{x_{M_g}}(f)$ and $\mathbf{C}^{\delta_i}_{x_{M_g}}(f)$ are the Fourier transforms of the first, $\mathbf{R}^{\gamma_i}_{x_{M_g}}(\tau)$, and second, $\mathbf{C}^{\delta_i}_{x_{M_g}}(\tau)$, cyclic correlation matrices of $\mathbf{x}_{M_g}(t)$ for the delay τ and the cyclic frequency γ_i and δ_i respectively. In the presence of MUI having same nature (R or QR), symbol period and carrier frequency as the SOI, it is straightforward to verify that for all the previous considered receivers ($M = 1, 2$; R and QR signals), $\gamma_i = \delta_i = \alpha_i = i/T$, $i \in \mathbb{Z}$. This implies that (34) (35) and then, $\text{SINR}_{M_g}(k)$, do not depend on k and $\text{SINR}_{M_g}(k)$ is simply denoted by SINR_{M_g}. Using (31) and (34) to (37) into (33), we obtain:

$$\text{SINR}_{M_g} = \frac{2\pi_b u^2_{M_g}}{\left\{\begin{array}{l}\sum_{\alpha_i} \int [\mathbf{w}^H_{M_g}(f+\alpha_i/2)\mathbf{R}^{\alpha_i}_{x_{M_g}}(f)\mathbf{w}_{M_g}(f-\alpha_i/2) \\ +\text{Re}(\mathbf{w}^H_{M_g}(f+\alpha_i/2)\mathbf{C}^{\alpha_i}_{x_{M_g}}(f)\mathbf{w}^*_{M_g}(\alpha_i/2-f))]df\end{array}\right. - 2\pi_b u^2_{M_g}}, \quad (38)$$

where $u_{M_g} \stackrel{\text{def}}{=} \int \mathbf{w}^H_{M_g}(f)\mathbf{g}_{M_g}(f)df$. As for $M = 2$, it is straightforward to prove that $y_{M_g}(k)$ is real-valued whatever the considered receiver, SINR_{2_g} reduces in this case to:

$$\text{SINR}_{2_g} = \frac{\pi_b[\int \mathbf{w}^H_{2_g}(f)\mathbf{g}_{2_g}(f)df]^2}{\left\{\begin{array}{c}\sum_{\alpha_i} \int \mathbf{w}^H_{2_g}(f+\alpha_i/2)\mathbf{R}^{\alpha_i}_{x_{2_g}}(f)\mathbf{w}_{2_g}(f-\alpha_i/2)df \\ -\pi_b[\int \mathbf{w}^H_{2_g}(f)\mathbf{g}_{2_g}(f)df]^2\end{array}\right.}. \quad (39)$$

For the MMSE (o) receiver, it is proved in Appendix A that (38) and (39) can be written as a function of the only matrix $\mathbf{C}^d_M(f)$ and vector $\mathbf{f}$ defined after (10), which gives

$$\text{SINR}_{M_o} = \frac{2\pi_b[1 - \frac{N_0T}{\pi_b}\int_\Delta \mathbf{f}^T\mathbf{C}^d_M(f)\mathbf{f}df]^2}{\left\{\begin{array}{l}N_0T\int_\Delta \mathbf{f}^T\mathbf{C}^d_M(f)\mathbf{f}df - \frac{2(N_0T)^2}{\pi_b}(\int_\Delta \mathbf{f}^T\mathbf{C}^d_M(f)\mathbf{f}df)^2 \\ +\frac{N_0^2T}{\pi_b}\int_\Delta \text{Re}[\mathbf{f}^T\mathbf{C}^d_M(f)\mathbf{C}^{d^*}_M(-f)\mathbf{f}]df \\ +\delta(M-2)[N_0T\int_\Delta \mathbf{f}^T\mathbf{C}^d_M(f)\mathbf{f}df \\ -\frac{N_0^2T}{\pi_b}\int_\Delta \mathbf{f}^T\mathbf{C}^d_M(f)\mathbf{C}^d_M(f)\mathbf{f}df]\end{array}\right.} \quad (40)$$

$$\text{SINR}_{2_o} = \frac{\pi_b}{N_0T\int_\Delta \mathbf{f}^T\mathbf{C}^d_M(f)\mathbf{f}df} - 1. \quad (41)$$

Following a similar approach, it is proved in Appendix B

[2]Note that for the (sc) receiver, $y_{M_g}(t)$ denotes from (23), the CT signal $\int c^d_{M_{sc}}(f)\mathbf{g}^d_{v,M}{}^H(f)[\mathbf{R}^d_{n_{v,M}}(f)]^{-1}\mathbf{x}_{v_M}(f)e^{i2\pi ft}df$.

that for the (s) receivers, (38) and (39) can be written as

$$\mathrm{SINR}_{M_s} = \frac{2\pi_b[1-\frac{T}{\pi_b}\int_\Delta c_M^d(f)df]^2}{\left\{\begin{array}{l}\frac{\pi_b}{T}\int_\Delta {c_M^d}^2(f)\big[\|\sum_\ell \mathbf{G}_M^H(f-\frac{\ell}{T})[\mathbf{R}_{n,M}^0(f-\frac{\ell}{T})]^{-1}\\ \mathbf{g}_M(f-\frac{\ell}{T})\|^2+\mathrm{Re}\{\sum_\ell\sum_k \mathbf{g}_M^H(f-\frac{\ell}{T})[\mathbf{R}_{n,M}^0(f-\frac{\ell}{T})]^{-1}\\ \mathbf{G}_M(f-\frac{\ell}{T})\mathbf{G}_M^T(-f-\frac{k}{T})[\mathbf{R}_{n,M}^{0^*}(-f-\frac{k}{T})]^{-1}\mathbf{g}_M^*(-f-\frac{k}{T})\}\big]df\\ -2\pi_b[1-\frac{T}{\pi_b}\int_\Delta c_M^d(f)df]^2\\ +(1+\delta(M-2))N_0T\int_\Delta c_M^d(f)(1-\frac{1}{\pi_b}c_M^d(f))df\end{array}\right.} \quad (42)$$

$$\mathrm{SINR}_{2_s} = \frac{\pi_b[1-\frac{T}{\pi_b}\int_\Delta c_M^d(f)df]^2}{\left\{\begin{array}{l}\frac{\pi_b}{T}\int_\Delta {c_M^d}^2(f)\|\sum_\ell \mathbf{G}_M^H(f-\frac{\ell}{T})[\mathbf{R}_{n,M}^0(f-\frac{\ell}{T})]^{-1}\\ \mathbf{g}_M(f-\frac{\ell}{T})\|^2-\pi_b[1-\frac{T}{\pi_b}\int_\Delta c_M^d(f)df]^2\\ +N_0T\int_\Delta c_M^d(f)(1-\frac{1}{\pi_b}c_M^d(f))df\end{array}\right.} \quad (43)$$

Finally, as $\mathbf{x}_{v,M}(nT)$ (17) and $y_{M_{sc}}(k)$ (23) are SO stationary, it is proved in Appendix C that for the (sc) receivers, (38) and (39) can be written as

$$\mathrm{SINR}_{M_{sc}} = \frac{2\pi_b T[\int_\Delta \mathbf{g}_{v_M}^{d^H}(f)[\mathbf{R}_{x_{v_M}}^d(f)]^{-1}\mathbf{g}_{v_M}^d(f)df]^2}{\left\{\begin{array}{l}\int_\Delta \mathbf{g}_{v_M}^{d^H}(f)[\mathbf{R}_{x_{v_M}}^d(f)]^{-1}\mathbf{g}_{v_M}^d(f)df\\ +\mathrm{Re}[\int_\Delta \mathbf{g}_{v_M}^{d^H}(f)[\mathbf{R}_{x_{v_M}}^d(f)]^{-1}\mathbf{C}_{x_{v_M}}^d(f)[\mathbf{R}_{x_{v_M}}^{d^*}(-f)]^{-1}\\ \mathbf{g}_{v_M}^{d^*}(-f)df]-2\pi_b T[\int_\Delta \mathbf{g}_{v_M}^{d^H}(f)[\mathbf{R}_{x_{v_M}}^d(f)]^{-1}\mathbf{g}_{v_M}^d(f)df]^2\end{array}\right.} \quad (44)$$

$$\mathrm{SINR}_{2_{sc}} = \frac{\pi_b T\int_\Delta \mathbf{g}_{v_2}^{d^H}(f)[\mathbf{R}_{x_{v_2}}^d(f)]^{-1}\mathbf{g}_{v_2}^d(f)df}{1-\pi_b T\int_\Delta \mathbf{g}_{v_2}^{d^H}(f)[\mathbf{R}_{x_{v_2}}^d(f)]^{-1}\mathbf{g}_{v_2}^d(f)df}, \quad (45)$$

when $v(f)\neq 0$ in Δ which ensures that $\mathbf{R}_{x_{v_M}}^d(f)$ is not singular in Δ.

C. SINR analysis for zero or one MUI

C1) *Observation model and statistics:* We assume in this section that the total noise $\mathbf{n}(t)$ is composed of a background noise and, at most, one MUI, which generates the observation model (1) with $P=1$. In this context, the purpose of this section is to compute and compare the SINR at the output of the previous L and WL MMSE receivers for both R and QR signals. Note that, due to lack of space, comparison of the previous receivers from a SER criterion are presented in the companion paper [50]. From (1), for both R and QR signals, for all the previous considered receivers and for $M=1,2$, the matrices $\mathbf{R}_{x_{M_g}}^{\alpha_i}(f)$ and $\mathbf{C}_{x_{M_g}}^{\alpha_i}(f)$ appearing in (38) can be written from [48] as

$$\begin{aligned}\mathbf{R}_{x_{M_g}}^{\alpha_i}(f) &= \frac{\pi_b}{T}[\mathbf{g}_{M_g}(f+\alpha_i/2)\mathbf{g}_{M_g}^H(f-\alpha_i/2)\\ &\quad+\mathbf{g}_{1,M_g}(f+\alpha_i/2)\mathbf{g}_{1,M_g}^H(f-\alpha_i/2)]+\mathbf{R}_{\epsilon_{M_g}}^{\alpha_i}(f) \quad (46)\\ \mathbf{C}_{x_{M_g}}^{\alpha_i}(f) &= \frac{\pi_b}{T}[\mathbf{g}_{M_g}(f+\alpha_i/2)\mathbf{g}_{M_g}^T(\alpha_i/2-f)\\ &\quad+\mathbf{g}_{1,M_g}(f+\alpha_i/2)\mathbf{g}_{1,M_g}^T(\alpha_i/2-f)]+\mathbf{C}_{\epsilon_{M_g}}^{\alpha_i}(f) \quad (47)\end{aligned}$$

Here, $\mathbf{g}_{1,M_g}(f)=\mathbf{g}_{1,M}(f)$ for $g=o$ or s, whereas $\mathbf{g}_{1,M_g}(f)=\mathbf{g}_{1,v_M}(f)$ for $g=sc$. Moreover, $\mathbf{R}_{\epsilon_{M_g}}^{\alpha_i}(f)$ and $\mathbf{C}_{\epsilon_{M_g}}^{\alpha_i}(f)$ are such that:

$$\begin{aligned}\mathbf{R}_{\epsilon_{M_o}}^{\alpha_i}(f) &= \mathbf{R}_{\epsilon_{M_s}}^{\alpha_i}(f)=N_0\delta(\alpha_i)\mathbf{I}_{MN}; \quad (48)\\ \mathbf{R}_{\epsilon_{M_{sc}}}^{\alpha_i}(f) &= N_0|v(f)|^2\delta(\alpha_i)\mathbf{I}_{MN}; \text{for R signals} \quad (49)\\ \mathbf{R}_{\epsilon_{M_{sc}}}^{\alpha_i}(f) &= N_0|v(f+1/4T)|^2\delta(\alpha_i)\mathbf{I}_N;\\ &\quad \text{for QR signals and } M=1 \quad (50)\\ \mathbf{R}_{\epsilon_{M_{sc}}}^{\alpha_i}(f)&=N_0\delta(\alpha_i)\begin{pmatrix}|v(f+1/4T)|^2\mathbf{I}_N & \mathbf{0}_N\\ \mathbf{0}_N & |v(-f+1/4T)|^2\mathbf{I}_N\end{pmatrix};\\ &\quad \text{for QR signals and } M=2 \quad (51)\\ \mathbf{C}_{\epsilon_{M_o}}^{\alpha_i}(f) &= \mathbf{C}_{\epsilon_{M_s}}^{\alpha_i}(f)=N_0\delta(\alpha_i)\delta(M-2)\mathbf{J}_{2N}; \quad (52)\\ \mathbf{C}_{\epsilon_{M_{sc}}}^{\alpha_i}(f) &= N_0|v(f)|^2\delta(\alpha_i)\delta(M-2)\mathbf{J}_{2N};\\ &\quad \text{for R signals} \quad (53)\\ \mathbf{C}_{\epsilon_{M_{sc}}}^{\alpha_i}(f) &= \mathbf{0}_N \text{ for QR signals and } M=1 \quad (54)\\ \mathbf{C}_{\epsilon_{M_{sc}}}^{\alpha_i}(f)&=N_0\delta(\alpha_i)\begin{pmatrix}\mathbf{0}_N & |v(f+1/4T)|^2\mathbf{I}_N\\ |v(-f+1/4T)|^2\mathbf{I}_N & \mathbf{0}_N\end{pmatrix};\\ &\quad \text{for QR signals and } M=2 \quad (55)\end{aligned}$$

where N_0 is the power spectral density of each component of the background noise $\epsilon(t)$.

C2) *SINR analysis in the absence of interference:* To get more insights into the comparative behavior of the M-input MMSE receivers ($M=1,2$) for R and QR signals, we assume in this section an absence of MUI interference and a two-tap frequency selective channel such that

$$\mathbf{h}(t)=\mu_1\delta(t)\mathbf{h}_1+\mu_2\delta(t-\tau)\mathbf{h}_2. \quad (56)$$

Here μ_1 and μ_2 ($0\leq\mu_2\leq\mu_1$) control the amplitude of the first and second paths of the SOI respectively, τ is the delay between the two paths and $\mathbf{h}_1$ and $\mathbf{h}_2$, deterministic or random, with components $h_1(i)$ and $h_2(i)$, $i=1,..,N$, respectively, and such that $\mathrm{E}|h_1^2(i)|=\mathrm{E}|h_2^2(i)|=1$, correspond to the channel vectors of the two paths, respectively. Using (56) into (1), we deduce that the mean SOI symbol energy per antenna, E_s, can be written as

$$\begin{aligned}E_s &= \frac{\pi_b}{N}\int \mathrm{E}(\|\mathbf{g}^2(t)\|)dt\\ &= \pi_b\mu_1^2\left[1+\beta^2+2\beta\mathrm{Re}\left(\mathrm{E}\left(\mathbf{h}_1^H\mathbf{h}_2/N\right)\right)r_v(\tau)\right], \quad (57)\end{aligned}$$

where $\beta\overset{\mathrm{def}}{=}\mu_2/\mu_1$ is the selectivity coefficient of the channel and $r_v(t)\overset{\mathrm{def}}{=}v(t)\otimes v^*(-t)$. Denoting by $\alpha_{1,2}\overset{\mathrm{def}}{=}\mathbf{h}_1^H\mathbf{h}_2/(\|\mathbf{h}_1\|\|\mathbf{h}_2\|)$ the spatial correlation coefficient between $\mathbf{h}_1$ and $\mathbf{h}_2$ and assuming that, in the random case, $\mathbf{h}_1$ and $\mathbf{h}_2$ are statistically independent, expression (57) becomes

$$\begin{aligned}E_s &= \pi_b\mu_1^2[1+\beta^2+2\beta\mathrm{Re}(\alpha_{1,2})r_v(\tau)];\\ &\quad \text{in the deterministic case,} \quad (58)\\ &= \pi_b\mu_1^2(1+\beta^2); \text{ in the random case.} \quad (59)\end{aligned}$$

For a propagation channel with no delay spread ($\beta=0$),

for both $M = 1$ and $M = 2$, for both R and QR signals, as mentioned in (27), the three receivers (o), (s) and (sc) are equivalent and the expected value, $\mathrm{E}[\mathrm{SINR}_{M_g}]$, of the SINR at the output of these receivers, SINR_{M_g}, which corresponds to SINR_{M_g} for deterministic channels, is maximal and given by

$$\mathrm{E}[\mathrm{SINR}_{M_g}] = \frac{2NE_s}{N_0} \overset{\text{def}}{=} 2\epsilon_s. \tag{60}$$

Moreover, for both $M = 1$ and $M = 2$, for both R and QR signals, the three receivers (o), (s) and (sc) are also equivalent in the two following situations:

- for R, $\pi/2$-BPSK and $\pi/2$-ASK SOI and arbitrary propagation channel, when $v(t)$ is a square-root raised cosine filter with a zero roll-off, as stated by (28).
- for OQAM SOI, when $v(t)$ is a square-root raised cosine filter with an arbitrary roll-off, as stated by (28).

Excepted the two previous situations, for both $M = 1$ and $M = 2$, for both R and QR signals, the (sc) receiver (26) becomes sub-optimal with respect to the two other receivers and it has been verified by computer simulations that this sub-optimality increases with the SOI bandwidth (and thus with the roll-off for raised-cosine filters), the channel selectivity β, the modulus, $\alpha \overset{\text{def}}{=} |\alpha_{1,2}|$, of the spatial correlation coefficient between $\mathbf{h}_1$ and $\mathbf{h}_2$. Besides, this sub-optimality is more pronounced for deterministic than for random channels. To quantify and illustrate this sub-optimality of the (sc) receivers, we assume now that (τ, ϕ) are r.v. uniformly distributed on $[0, 4T] \times [0, 2\pi]$. Under these assumptions, choosing $N = 1$ (and thus $\alpha = 1$) and ϵ_s = 10 dB, Figs.4 and 5 show, for R and $\pi/2$-ASK QR signals respectively, for $M = 1, 2$, $\omega = 1$, $\beta = 1$ and deterministic channels, the variations of the estimated complementary cumulative distribution function $\Pr[(\mathrm{SINR}_{M_g}/2\epsilon_s)\mathrm{dB} \geq x\mathrm{dB}] \overset{\text{def}}{=} P_{M_g}(x)$ as a function of x (dB). Note that the curves appearing in these figures have been obtained from 10^5 Monte Carlo simulations where SINR_{M_g} have been computed from (38) to (39).

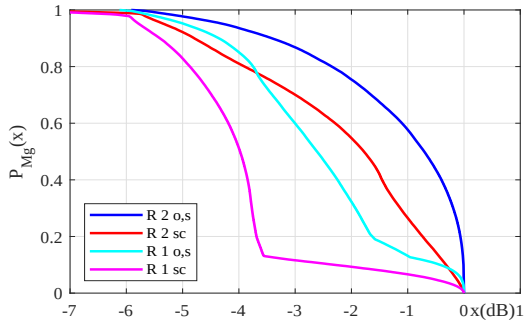

Fig. 4. $P_{M_g}(x)$ as a function of x ($N = 1$, $M = 1, 2$, $\epsilon_s = 10$ dB, $\omega = 1$, $\beta = 1$, deterministic channels, R signals)

We note the sub-optimality of the (sc) receivers for both $M = 1, 2$ and for both R and QR signals. Note also the better performance of WL receivers with respect to linear ones due to the phase discrimination exploitation of the two paths. Note finally the similar performance for R and QR signals for $M = 1$ but, for $M = 2$, the slightly better performance of (o) receiver for QR signals. To complete these results, Figs.6 and 7 show the same variations as Figs.4 and 5 under the same assumptions but for Rayleigh fading channels for which $h_1(1)$ and $h_2(1)$ are i.i.d. random variables following a zero-mean circular Gaussian distribution. The conclusion of Figs.4 and 5 hold for Figs.6 and 7 with a lower sub-optimality of the (sc) receivers and similar performance of (o) receiver for R and QR signals.

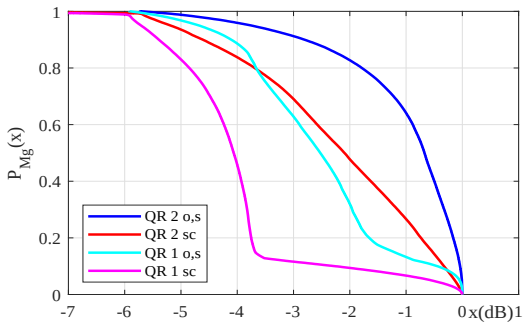

Fig. 5. $P_{M_g}(x)$ as a function of x ($N = 1$, $M = 1, 2$, $\epsilon_s = 10$ dB, $\omega = 1$, $\beta = 1$, deterministic channels, $\pi/2$-ASK QR signals).

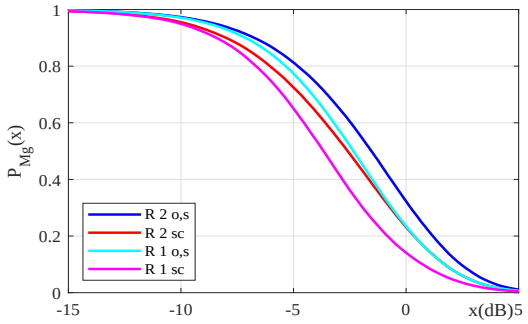

Fig. 6. $P_{M_g}(x)$ as a function of x ($N = 1$, $M = 1, 2$, $\epsilon_s = 10$ dB, $\omega = 1$, $\beta = 1$, random channels, R signals).

Finally note that for $M = 2$, interpretable closed-form expressions are possible when $\tau = \ell T$ where $\ell \in \mathbb{Z}^*$ in (56) where the SINR at the output of the (o) and (s) receivers for arbitrary roll-off are equal to the SINR at the output of the (sc) receiver for a zero roll-off, for which we get

$$\begin{aligned} \mathrm{SINR}_{R_{2,o}} &= \mathrm{SINR}_{R_{2,s}} = \mathrm{SINR}_{R_{2,sc}} \\ \mathrm{SINR}_{QR_{2,o}} &= \mathrm{SINR}_{QR_{2,s}} = \mathrm{SINR}_{QR_{2,sc}} \\ &= (1+2\epsilon_s)\left(\frac{1-\gamma^2}{1+\gamma^2}\right) - 1 \text{ for } \beta \neq 0 \\ &= 2\epsilon_s \qquad\qquad \text{for } \beta = 0 \end{aligned} \tag{61}$$

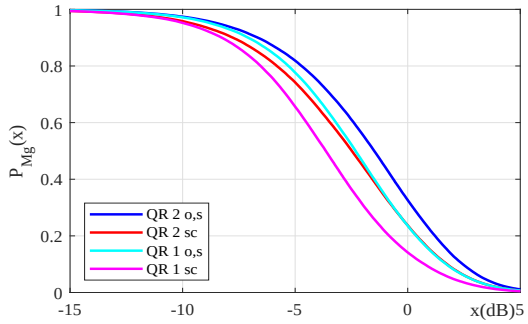

Fig. 7. $P_{M_g}(x)$ as a function of x ($N=1$, $M=1,2$, $\epsilon_s=10$ dB, $\omega=1$, $\beta=1$, random channels, $\pi/2$-ASK QR signals).

where for $\beta \neq 0$:

$$\begin{aligned}\gamma &= \frac{(1+2\epsilon_s)(1+\beta^2)}{4\beta\epsilon_s\alpha\cos\phi}\left(1-\sqrt{1-\frac{16\beta^2\epsilon_s^2\alpha^2\cos^2\phi}{(1+2\epsilon_s)^2(1+\beta^2)^2}}\right) \\ &\quad \text{for } \alpha\cos\phi\neq 0 \\ &= 0 \qquad \text{for } \alpha\cos\phi = 0 \end{aligned} \tag{62}$$

where $\phi=\mathrm{Arg}(\alpha_{1,2})$ and $\phi=\mathrm{Arg}(\alpha_{1,2})+\ell\pi/2$ for R and QR signals respectively. We clearly see that these SINR are decreasing when the spatial correlation α increases and that these SINR tend to $2\epsilon_s$ for β and $\alpha\cos\phi$ tending to zero for which γ tends to zero in (62).

C3) *SINR analysis for one MUI and channels with no delay spread:*

a) *Propagation model*

To analyze the comparative behavior of the M-input MMSE receivers ($M=1,2$), for R and QR signals, in the presence of interference, we assume in this section the presence of one MUI and propagation channels with no delay spread such that

$$\mathbf{h}(t)=\mu\delta(t)\mathbf{h} \quad \text{and} \quad \mathbf{h}_1(t)=\mu_1\delta(t-\tau_1)\mathbf{h}_1. \tag{63}$$

Here μ and μ_1 control the amplitude of the SOI and MUI respectively and τ_1 is the delay of the MUI with respect to the SOI. The vectors $\mathbf{h}$ and $\mathbf{h}_1$, random or deterministic, with components $h(i)$ and $h_1(i)$, $1\leq i\leq N$, respectively and such that $\mathrm{E}[|h(i)|^2]=\mathrm{E}[|h_1(i)|^2]=1$, $1\leq i\leq N$, correspond to the channel vectors of the SOI and MUI, respectively. Similarly as (58) and (59), the mean SOI and MUI energy per antenna, E_s and E_1 respectively are given by $E_s=\pi_b\mu^2$ and $E_1=\pi_{b_1}\mu_1^2$, where $\pi_{b_1}\overset{\text{def}}{=}\mathrm{E}(b_{1,k}^2)$. We then denote by ϵ and ϵ_1 the quantities $\epsilon_s\overset{\text{def}}{=}E_s\ \mathrm{E}(\|\mathbf{h}\|^2)/N_0=NE_s/N_0$ and $\epsilon_1\overset{\text{def}}{=}E_1\ \mathrm{E}(\|\mathbf{h}_1\|^2)/N_0=NE_1/N_0$.

b) *Deterministic channels and zero roll-off*

Under the previous assumptions, analytical interpretable expressions of SINR_{M_g} defined by (38) and (39) are only possible for a square root raised cosine (SRRC) filter $v(t)$ for the symbol duration T with a zero roll-off ω, i.e., for R, $\pi/2$-BPSK and $\pi/2$-ASK constellations with $\omega=0$, which is assumed in this subsection. Otherwise, the computation of SINR_{M_g} can only be done numerically by computer simulations and will be discussed in the following subsections. Moreover, we assume in this subsection deterministic channels and we denote by $\alpha_{s,1}\overset{\text{def}}{=}|\alpha_{s,1}|e^{j\phi_{s,1}}$ the spatial correlation coefficient between the SOI and the MUI, such that $0\leq|\alpha_{s,1}|\leq 1$, and defined similarly as $\alpha_{1,2}$ by replacing $\mathbf{h}_1$ and $\mathbf{h}_2$ by $\mathbf{h}$ and $\mathbf{h}_1$, respectively. Finally, we denote by $\mathrm{SINR}_{R_{M_g}}$ and $\mathrm{SINR}_{QR_{M_g}}$ the SINR (38) at the output of the M-input MMSE receivers ($M=1,2$), for R and QR signals respectively.

When $|\alpha_{s,1}|\neq 1$, i.e., when there exists a spatial discrimination between the SOI and the MUI (which requires $N>1$), assuming a strong MUI ($\epsilon_1\gg 1$), we obtain from (38) and (39) after cumbersome derivations, the following expressions:

$$\begin{aligned}\mathrm{SINR}_{R_{1,o}} &= \mathrm{SINR}_{R_{1,s}}=\mathrm{SINR}_{R_{1,sc}} \\ &\approx \mathrm{SINR}_{QR_{1,o}}=\mathrm{SINR}_{QR_{1,s}}=\mathrm{SINR}_{QR_{1,sc}} \\ &\approx 2\epsilon_s(1-|\alpha_{s,1}|^2) \end{aligned} \tag{64}$$

$$\begin{aligned}\mathrm{SINR}_{R_{2,o}} &= \mathrm{SINR}_{R_{2,s}}=\mathrm{SINR}_{R_{2,sc}} \\ &\approx 2\epsilon_s(1-|\alpha_{s,1}|^2\cos^2\phi_{s,1}) \end{aligned} \tag{65}$$

$$\mathrm{SINR}_{QR_{2,o}}=\mathrm{SINR}_{QR_{2,sc}}\approx 2\epsilon_s\left(1-\frac{|\alpha_{s,1}|^2}{2}\right.$$
$$\left.\frac{(1+2\epsilon_s)(\cos^2\zeta_{s,1}+\cos^2\psi_{s,1})-4|\alpha_{s,1}|^2\epsilon_s\cos^2\zeta_{s,1}\cos^2\psi_{s,1}}{(1+2\epsilon_s)-|\alpha_{s,1}|^2\epsilon_s(\cos^2\zeta_{s,1}+\cos^2\psi_{s,1})}\right) \tag{66}$$

which reduces to (65) for synchronous SOI and MUI ($\tau_1=0$).

$$\mathrm{SINR}_{QR_{2,s}} \approx 2\epsilon_s\left(1-\frac{|\alpha_{s,1}|^2}{2}\right.$$
$$\left.\frac{1+\cos^2\psi_{s,1}+2\epsilon_s(1+\cos^2\psi_{s,1}(1-2|\alpha_{s,1}|^2))}{1+\epsilon_s(2-|\alpha_{s,1}|^2(1+\cos^2\psi_{s,1}))}\right), \tag{67}$$

where $\psi_{s,1}\overset{\text{def}}{=}\phi_{s,1}-\pi\tau_1/2T$ and $\zeta_{s,1}\overset{\text{def}}{=}\phi_{s,1}+\pi\tau_1/2T$. We deduce from (65) to (67) that $\mathrm{SINR}_{R_{2,g}}/\epsilon_s$ does not depend on ϵ_s while $\mathrm{SINR}_{QR_{2,g}}/\epsilon_s$ depends on ϵ_s, which proves the absence (for R signals) and the presence (for QR signals) of ISI in the output $z_{2_g}(k)$.

However, when $|\alpha_{s,1}|=1$, i.e., when there is no spatial discrimination between the SOI and the MUI, which is in particular the case for $N=1$, after tedious computations, we obtain, for $M=1$

$$\begin{aligned}\mathrm{SINR}_{R_{1,o}} &= \mathrm{SINR}_{R_{1,s}}=\mathrm{SINR}_{R_{1,sc}} \\ &= \frac{2\epsilon_s}{1+2\epsilon_1\cos^2\phi_{s,1}} \end{aligned} \tag{68}$$

$$\begin{aligned}\mathrm{SINR}_{QR_{1,o}} &= \mathrm{SINR}_{QR_{1,s}}=\mathrm{SINR}_{QR_{1,sc}} \\ &= \frac{2\epsilon_s}{1+\epsilon_1(\cos^2\psi_{s,1}+\cos^2\zeta_{s,1})}, \end{aligned} \tag{69}$$

whereas, assuming a strong MUI ($\epsilon_1\gg 1$), we obtain, for

$M = 2$

$$\begin{aligned}
\mathrm{SINR}_{R_{2,o}} &= \mathrm{SINR}_{R_{2,s}} = \mathrm{SINR}_{R_{2,sc}} \\
&\approx 2\epsilon_s(1-\cos^2\phi_{s,1}), \text{for } \phi_{s,1} \neq k\pi \quad (70) \\
&= \frac{2\epsilon_s}{1+2\epsilon_1}, \qquad \text{for } \phi_{s,1} = k\pi \quad (71) \\
\mathrm{SINR}_{QR_{2,o}} &= \mathrm{SINR}_{QR_{2,sc}} \approx 2\epsilon_s\,(1- \\
&\frac{(1+2\epsilon_s)(\cos^2\zeta_{s,1}+\cos^2\psi_{s,1})-4\epsilon_s\cos^2\zeta_{s,1}\cos^2\psi_{s,1}}{2[1+2\epsilon_s-\epsilon_s(\cos^2\zeta_{s,1}+\cos^2\psi_{s,1})]}\Big), \\
&\qquad \text{for } (\psi_{s,1},\zeta_{s,1}) \neq (k_1\pi, k_2\pi), \quad (72) \\
&\approx \frac{\epsilon_s}{\epsilon_1}, \text{ for } (\psi_{s,1},\zeta_{s,1}) = (k_1\pi, k_2\pi), \quad (73)
\end{aligned}$$

Note that (72) reduces to (70) for synchronous SOI and MUI ($\tau_1 = 0$).

$$\begin{aligned}
\mathrm{SINR}_{QR_{2,s}} &\approx 2\epsilon_s\left(1-\frac{1+\cos^2\psi_{s,1}+2\epsilon_s(1-\cos^2\psi_{s,1})}{2[1+\epsilon_s(1-\cos^2\psi_{s,1})]}\right)= \\
&\frac{\epsilon_s\sin^2\psi_{s,1}}{1+\epsilon_s\sin^2\psi_{s,1}}, \text{ for } \psi_{s,1} \neq k\pi \quad (74) \\
&\approx \frac{9\epsilon_s}{2\epsilon_1(1+4\cos^2\zeta_{s,1})}, \text{ for } \psi_{s,1} = k\pi \quad (75)
\end{aligned}$$

A receiver performs MAIC (for $N > 1$) or SAIC (for $N = 1$) as $\epsilon_1 \to \infty$, if the associated SINR does not converge toward zero. We deduce from (64), (68) and (69) that, for both R and QR signals, the conventional receivers ($M = 1$) perform MAIC as soon as $|\alpha_{s,1}| \neq 1$, but perform SAIC very scarcely, only when $\phi_{s,1} = (2k+1)\pi/2$ for R signals and when $(\tau_1/T, \phi_{s,1}) = (2k_1, (2k_2+1)\pi/2)$ or $(2k_1+1, k_2\pi)$ for QR signals, where k, k_1 and k_2 are integers. Moreover, we deduce from (65) to (67) and (70) to (75) that, for both R and QR signals, the three two-input MMSE receivers perform MAIC as soon as $|\alpha_{s,1}| \neq 1$, but perform SAIC as long as $\phi_{s,1} \neq k\pi$ for R signals, $(\psi_{s,1}, \zeta_{s,1}) \neq (k_1\pi, k_2\pi)$ for QR signals and receivers (o) and (sc) and $\psi_{s,1} \neq k\pi$ for QR signals and receiver (s), enlightening the great interest of the three two-input WL MMSE receivers in both cases. Moreover, we deduce from equations (64), (65), (68) and (70) that for R signals, for both $M = 1$ and $M = 2$, the three MMSE (o), (s), (sc) receivers are equivalent, discarding in this case the need to estimate the channel of the MUI and proving that the structure constraint has no impact on performance. Expression (64) shows that the equivalence of the three receivers also holds for QR signal for $M = 1$ as long as there is a spatial discrimination between the SOI and the MUI. However, despite similar processing and similar extended models (6) and (8) for R and QR signals respectively, the output SINRs (65) and (66), (67), for $|\alpha_{s,1}| \neq 1$, and (68), (70), (71) and (69), (72) to (75) for $|\alpha_{s,1}| = 1$, correspond to different expressions. This proves the general non equivalence of R and derotated QR signals for the three WL MMSE receivers in the presence of MUI, result which has already been obtained for pseudo-ML receivers [48]. In particular, for a zero roll-off, while (65), only depends on $2\epsilon_s$: the maximum output SINR obtained without interference, and the parameters $\alpha_{s,1}$ and $\phi_{s,1}$, (66) and (67) depends not only on the previous parameters but also on τ_1/T. Note that the only equivalence between R and QR signals is obtained for synchronous SOI and MUI for the (o) and (sc) receivers. Moreover, (66), (67), (72) to (75) show that for QR signals and a zero roll-off, the WL MMSE receiver s becomes sub-optimal with respect to WL MMSE receivers o and sc, which are both equivalent in this case.

To illustrate the previous results, Figs.8a and 8b show, for the three receivers, the variations of $\mathrm{SINR}_{R_{M_g}}$ and $\mathrm{SINR}_{QR_{M_g}}$ ($M = 1, 2$) as a function of $\phi_{s,1}$ for $N = 1$, ϵ_s = 0 dB (a), ϵ_s = 15 dB (b), ϵ_1 = 20 dB for synchronous ($\tau_1 = 0$) SOI and MUI. Contrary to the conventional receiver, we note a SAIC capability of the WL MMSE receivers for both R and QR signals as soon as there is a phase discrimination between the sources. We note equivalent performance of the three WL MMSE receivers for R signals and of the WL MMSE receivers (o) and (sc) for QR signals but suboptimal performance of the WL MMSE (s) receiver for QR signals.

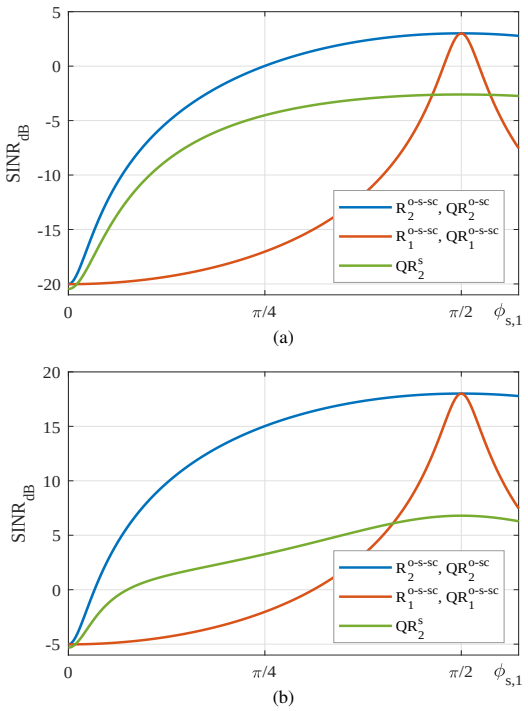

Fig. 8. $\mathrm{SINR}_{R_{M_g}}$ and $\mathrm{SINR}_{QR_{M_g}}$ as a function of $\phi_{s,1}$ ($N = 1$, $M = 1, 2$, ϵ_s =0 dB (a), ϵ_s = 15 dB (b) ϵ_1 = 20 dB, $\tau_1 = 0$, $\omega = 0$ deterministic channels.)

c) *Deterministic channels and arbitrary roll-off*

To compare the performance of the three MMSE receivers for R and QR signals, $\omega = 0$ and arbitrary values of τ_1 and also to extend the analysis to arbitrary values of the roll-off

ω, we must adopt a statistical perspective. For this purpose, we still consider deterministic channels and we assume that $(\phi_{s,1}, \tau_1)$ are r.v. uniformly distributed on $[0, 2\pi] \times [0, 4T]$. Under these assumptions, choosing ϵ_s = 10 dB and ϵ_1 = 20 dB, Figs.9/10 and 11/12 show, for R and QR signals respectively, for $N = 1$, $M = 1, 2$ and $\omega = 0$, the variations of $\Pr[(\text{SINR}_{M_g}/2\epsilon_s)\text{dB} \geq x\text{dB}] \stackrel{\text{def}}{=} P_{M_g}(x)$ as a function of x (dB). Figs.13 and 14 show the same variations as Figs.10 and 12, but for $\omega = 1$.

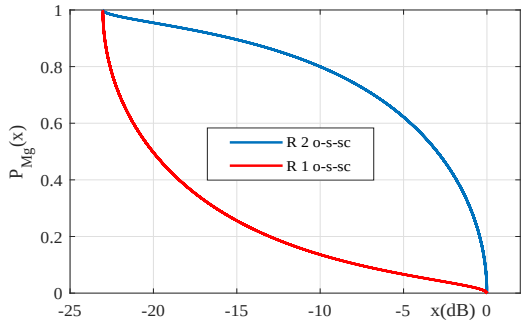

Fig. 9. $\text{P}_{M_g}(x)$ as a function of x ($N = 1$, $M = 1, 2$, ϵ_s = 10 dB, ϵ_1 = 20 dB, $\omega = 0$, deterministic channels, R signals) computed from closed-form expressions of the SINR without any integral.

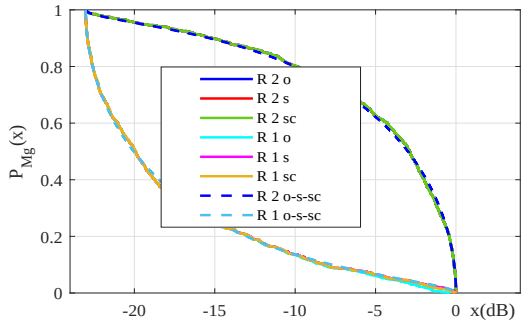

Fig. 10. $\text{P}_{M_g}(x)$ as a function of x ($N = 1$, $M = 1, 2$, ϵ_s = 10 dB, ϵ_1 = 20 dB, $\omega = 0$, deterministic channels, R signals). The two dashed curves correspond to the two solid curves of Fig. 9.

Note, for both R and QR signals, poor performance whatever ω for $M = 1$, i.e., for the conventional receiver. Note for $M = 2$ and R signals, quasi-optimal performance of the receivers s and sc for low values of ω and a slight increasing sub-optimality of receivers (s) and (sc) as ω increases. Note for $M = 2$ and QR signals, quasi-optimal performance of the receiver (sc) for low values of ω, a slight increasing sub-optimality of receiver (sc) as ω increases and a sub-optimality of receiver (s) whatever the roll-off. This proves, for channels with no delay spread and arbitrary values of ω, the great interest of WL MMSE receivers (sc) and (s) for R signals and of WL MMSE receiver (sc) for QR signals. This proves also the necessity to improve receiver

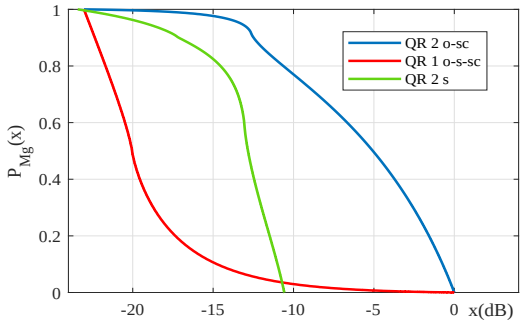

Fig. 11. $\text{P}_{M_g}(x)$ as a function of x ($N = 1$, $M = 1, 2$, ϵ_s = 10 dB, ϵ_1 = 20 dB, $\omega = 0$, deterministic channels, $\pi/2$-ASK QR signals) computed from closed-form expressions of the SINR without any integral.

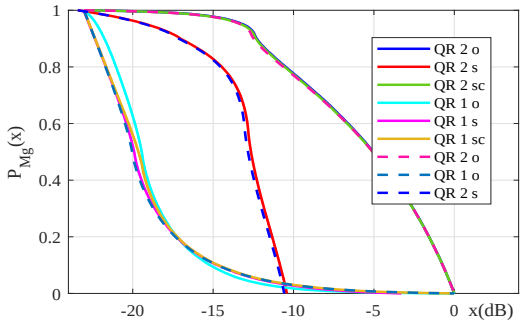

Fig. 12. $\text{P}_{M_g}(x)$ as a function of x ($N = 1$, $M = 1, 2$, ϵ_s = 10 dB, ϵ_1 = 20 dB, $\omega = 0$, deterministic channels, $\pi/2$-ASK QR signals). The three dashed curves correspond to three solid curves of Fig. 11.

(s) for QR signals, which will be done in the companion paper [50]. Due to lack of space, other illustrations of the same kind will be presented in the companion paper [50] for random channels and also for OQAM, MSK and GMSK signals.

V. Conclusion

New insights into linear and WL MMSE receivers have been given in this paper, for both R and QR signals, omnipresent in numerous present and future applications, in the absence and in the presence of data-like MUI and for propagation channels with or without delay spread. Several QR signals corresponding to $\pi/2$-BPSK, $\pi/2$-ASK and OQAM signals have been considered in this paper. Other QR signals corresponding to MSK and approximated GMSK signals will be considered in the companion paper [50]. Three concepts of Linear and WL MMSE receivers, corresponding to the optimal one (o), which optimally exploits the cyclostationarity properties of the signals, the one falsely assuming stationary MUI (s) and one with the structure constraint (sc) of most of receivers of the literature, have been considered and compared to each other. The (o) receivers require the a priori knowledge or estimation

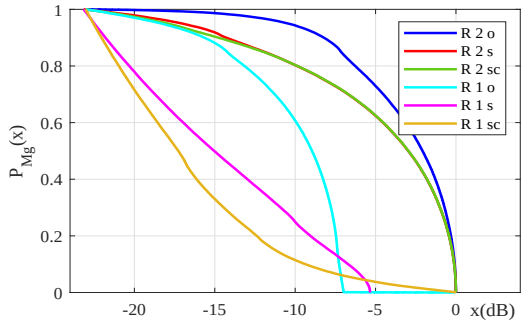

Fig. 13. $P_{M_g}(x)$ as a function of x ($N = 1$, $M = 1, 2$, ϵ_s = 10 dB, ϵ_1 = 20 dB, $\omega = 1$, deterministic channels, R signals).

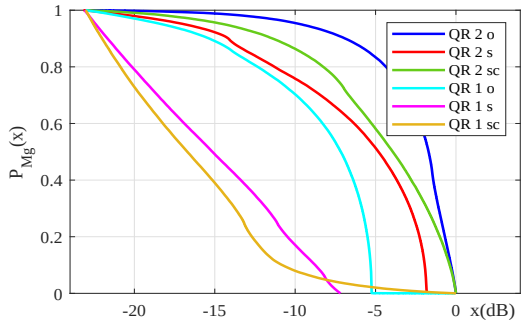

Fig. 14. $P_{M_g}(x)$ as a function of x ($N = 1$, $M = 1, 2$, ϵ_s = 10 dB, ϵ_1 = 20 dB, $\omega = 1$, deterministic channels, $\pi/2$-ASK QR signals).

of the channel of all the MUI, whereas the (s) and (sc) ones, a priori sub-optimal, only require the estimation of the SOI channel, hence their practical interest. A performance comparison of these three receivers has been presented both analytically and by computer simulations, using a CT approach for propagation channels with or without delay spread. In the absence of MUI, it has been shown the equivalence of the three receivers whatever the propagation channel for R, π/2-BPSK and π/2-ASK signals using a SRRC filter with a zero roll-off and for OQAM signals using a SRRC filter whatever the value of the roll-off. Otherwise and for most of frequency selective channels, the (sc) receiver is suboptimal with respect to the two others which coincide. In the presence of MUI, the three receivers are generally not equivalent, even for propagation channels with no delay spread for SRRC filters with non-zero roll-off. More precisely, for R signals using SRRC filters, WL receivers (s) and (sc) are quasi-optimal for weak values of the roll-off but their sub-optimality slightly increases with the roll-off. For QR signals using SRRC filters for the symbol duration T, such as π/2-BPSK, π/2-ASK signals, the previous results hold for the (sc) receiver only and the receiver (s) becomes clearly sub-optimal whatever the value of the roll-off. Other results will be presented in the companion paper [50] for other QR signals such as OQAM, MSK and GMSK signals. Taking into account the results both with and without interference and channels without and with delay spread, we conclude that contrary to the sc receivers, the WL s receiver are not far from the optimality for R signals and weak roll-off, discarding in this case the need to estimate the MUI channels. However this result does not hold for R signals and large roll-off and for QR signals, for which the WL s receiver is generally sub-optimal in the presence of MUI. For this reason, three-input WL MMSE s receivers are introduced in the companion paper [50], to make the WL receiver (s), which only requires the knowledge or estimation of the SOI channel, to become quasi-optimal for both R and QR signals, whatever the shaping filter.

APPENDIX

A. Proofs related to the optimal MMSE receivers

1) Proof of (10)*:* Noting that the joint MSE criterion (JMSE) satisfies $\mathrm{E}\|\mathbf{b}_k - \mathbf{y}_M(kT)\|^2 = \mathrm{E}|b_k - y_M(kT)|^2 + \sum_{p=1}^{P} \mathrm{E}|b_{p,k} - y_{M,p}(kT)|^2$ where $y_{M,p}(t) = \mathbf{w}_{M,p}^*(-t) \otimes \mathbf{x}_M(t)$ and $\mathbf{W}_M(f) = [\mathbf{w}_M(f), \mathbf{w}_{M,1}(f), .., \mathbf{w}_{M,p}(f), .., \mathbf{w}_{M,P}(f)]$, the optimal MMSE filter $\mathbf{w}_{M_o}(f)$ is the first column of the optimal joint MMSE filter $\mathbf{W}_{M_o}(f)$. The output, at time kT of the filter matrix $\mathbf{W}_M^*(f)$ corresponds to the SO stationary signal:

$$\mathbf{y}_M(k) = \mathbf{U}_M(0)\mathbf{b}_k + \sum_{\ell \neq k} \mathbf{U}_M(k-\ell)\mathbf{b}_\ell + \boldsymbol{\epsilon}_{w,M}(k), \quad (76)$$

where $\mathbf{U}_M(\ell) \overset{\text{def}}{=} \int \mathbf{W}_M^H(f)\mathbf{G}_M(f)e^{j2\pi f\ell T}df$ and $\boldsymbol{\epsilon}_{w,M}(k) \overset{\text{def}}{=} \int \mathbf{W}_M^H(f)\boldsymbol{\epsilon}_M(f)e^{j2\pi fkT}df$. Consequently the JMSE criterion is given by:

$$\begin{aligned}
\text{JMSE} &= \pi_b \mathrm{Tr}[(\mathbf{U}_M(0) - \mathbf{I}_{P+1})(\mathbf{U}_M(0) - \mathbf{I}_{P+1})^H] \\
&+ \pi_b \sum_{\ell \neq 0} \mathrm{Tr}[\mathbf{U}_M(\ell)\mathbf{U}_M^H(\ell)] \\
&+ \mathrm{Tr}[\mathrm{E}(\boldsymbol{\epsilon}_{w,M}(k)\boldsymbol{\epsilon}_{w,M}^H(k))] \\
&= \pi_b T \int_\Delta \mathrm{Tr}[(\mathbf{I}_{P+1} - \sum_\ell \mathbf{U}_M(\ell)e^{-j2\pi\ell fT}) \\
&\qquad (\mathbf{I}_{P+1} - \sum_\ell \mathbf{U}_M(\ell)^{-j2\pi\ell fT})^H]df \\
&+ \mathrm{Tr}[\mathrm{E}(\boldsymbol{\epsilon}_{w,M}(k)\boldsymbol{\epsilon}_{w,M}^H(k))] \\
&= \pi_b T \int_\Delta \mathrm{Tr}\big[\big(\mathbf{I}_{P+1} - \frac{1}{T}\sum_\ell \mathbf{W}_M^H(f - \frac{\ell}{T}) \\
&\mathbf{G}_M(f - \frac{\ell}{T})\big)\big(\mathbf{I}_{P+1} - \frac{1}{T}\sum_\ell \mathbf{W}_M^H(f - \frac{\ell}{T})\mathbf{G}_M(f - \frac{\ell}{T})\big)^H\big]df \\
&+ N_0 \int_\Delta \mathrm{Tr}\big[\sum_\ell \mathbf{W}_M^H(f - \frac{\ell}{T})\mathbf{W}_M(f - \frac{\ell}{T})\big]df, \quad (77)
\end{aligned}$$

where we have used the property $T\int_\Delta e^{-j2\pi\ell fT}df = \delta(0)$ in the fourth line. This JMSE is a quadratic functional of

$\mathbf{W}_M(f-\frac{k}{T})$, $k\in\mathbb{Z}$. Following a standard method of the calculus of variations (see e.g., [57]), the JMSE (77) is minimized by $\mathbf{W}_{M_o}(f)=\mathbf{G}_M(f)\mathbf{C}_M^d(f)$ where $\mathbf{C}_M^d(f)=\left[(N_0/\pi_b)\mathbf{I}_{P+1}+1/T\sum_\ell \mathbf{G}_M^H(f-\ell/T)\mathbf{G}_M(f-\ell/T)\right]^{-1}$. ■

2) Equivalence between the jointly and direct approaches: We consider here the MSE $\mathrm{E}|b_k-y_M(kT)|^2$ with $y_M(t)=\mathbf{w}_M^*(-t)\otimes\mathbf{x}_M(t)$ where the SO cyclostationarity of the MUI is taken into account. In this case, the CT total noise output $n_{M,w}(t)=\mathbf{w}_M^*(-t)\otimes\mathbf{n}_M(t)$ is SO cyclostationary with cyclic frequencies $\gamma_i=\alpha_i=i/T$ with power at times kT

$$\mathrm{E}[|n_{M,w}^2(k)|]=\sum_{\gamma_i}e^{j2\pi\gamma_i kT}\int r_{n_{M,w}}^{\gamma_i}df \tag{78}$$

with

$$r_{n_{M,w}}^{\gamma_i}(f)=\mathbf{w}_M^H(f+\gamma_i/2)\mathbf{R}_{n_M}^{\gamma_i}(f)\mathbf{w}_M(f-\gamma_i/2) \tag{79}$$

where

$$\begin{aligned}\mathbf{R}_{n_M}^{\alpha_i}(f) &= \sum_{1\le p\le P}\frac{\pi_b}{T}[\mathbf{g}_{p,M}(f+\alpha_i/2)\mathbf{g}_{p_M}^H(f-\alpha_i/2)\\ &+ N_0\delta(\alpha_i)\mathbf{I}_{MN}.\end{aligned} \tag{80}$$

Consequently

$$\begin{aligned}\mathrm{E}[|n_{M,w}^2(k)|] &= \frac{\pi_b}{T}\sum_{1\le p\le P}\sum_{\alpha_i}\int\mathbf{w}_M^H(f+\alpha_i/2)\\ &\mathbf{g}_{p,M}(f+\alpha_i/2)\mathbf{g}_{p_M}^H(f-\alpha_i/2)\mathbf{w}_M(f-\alpha_i/2)df\\ &+ N_0\int\|\mathbf{w}_M(f)\|^2df.\end{aligned} \tag{81}$$

This gives after direct algebraic manipulations, the following expressions of the MSE

$$\begin{aligned}\mathrm{MSE} &= \pi_bT\int_\Delta|1-\frac{1}{T}\sum_k\mathbf{w}_M^H(f-\frac{k}{T})\mathbf{g}_M(f-\frac{k}{T})|^2df\\ &+ \int_\Delta\frac{\pi_b}{T}\sum_{1\le p\le P}\sum_\ell\sum_k\mathbf{w}_M^H(f-\frac{k}{T})\\ &\mathbf{g}_{p,M}(f-\frac{k}{T})\mathbf{g}_{p,M}^H(f-\frac{\ell}{T})\mathbf{w}_M(f-\frac{\ell}{T})df\\ &+ N_0\int_\Delta\sum_k\|\mathbf{w}_M(f-\frac{k}{T})\|^2df.\end{aligned} \tag{82}$$

This MSE is a quadratic functional of $\mathbf{w}_M(f-\frac{k}{T})$, $k\in\mathbb{Z}$. Similarly to the JMSE, using a variational method, the MSE (82) is minimized by

$$\mathbf{w}_{M_o}(f)=c_{M,1}^d(f)\mathbf{g}_M(f)+\sum_{1\le p\le P}c_{M,1+p}^d(f)\mathbf{g}_{p,M}(f) \tag{83}$$

where $(c_{M,1}^d(f),c_{M,2}^d(f),..,c_{M,1+P}^d(f))^T$ is the first column of $\mathbf{C}_{M_o}^d(f)=[\frac{N_0}{\pi_b}\mathbf{I}_{P+1}+\frac{1}{T}\sum_\ell\mathbf{G}_M^H(f-\frac{\ell}{T})\mathbf{G}_M(f-\frac{\ell}{T})]^{-1}$. ■

3) Proof of (40) *and* (41)*:* The first component of $\mathbf{y}_M(k)$ (76) is given by

$$\begin{aligned}y_M(k) &= b_k(\mathbf{f}^T\mathbf{U}_{M_o}(0)\mathbf{f})+\mathbf{f}^T\mathbf{U}_{M_o}(0)(\mathbf{b}_k-b_k\mathbf{f})\\ &+ \sum_{\ell\neq k}\mathbf{f}^T\mathbf{U}_{M_o}(k-\ell)\mathbf{b}_\ell+\mathbf{f}^T\boldsymbol{\epsilon}_{w,M}(k)\\ &\stackrel{\mathrm{def}}{=} b_k(\mathbf{f}^T\mathbf{U}_{M_o}(0)\mathbf{f})+e_M(k),\end{aligned} \tag{84}$$

where b_k and $e_M(k)$ are uncorrelated and $\mathbf{U}_{M_o}(0)$ is given from the definition of $\mathbf{C}_M^d(f)$ in $\mathbf{w}_{M_o}(f)$ (10) by

$$\begin{aligned}\mathbf{U}_{M_o}(0) &= \int_\Delta\mathbf{C}_M^d(f)\sum_\ell\mathbf{G}_M^H(f-\frac{\ell}{T})\mathbf{G}_M(f-\frac{\ell}{T})df\\ &= \mathbf{I}_{P+1}-\frac{N_0T}{\pi_b}\int_\Delta\mathbf{C}_M^d(f)df.\end{aligned} \tag{85}$$

Noting that $\mathbf{U}_{M_o}(0)$ is Hermitian, the expressions of $\mathrm{E}(|e_M(k)|^2)$ and $\mathrm{E}(e_M^2(k))$ are given by:

$$\begin{aligned}\mathrm{E}(|e_M(k)|^2) &= \pi_b\mathbf{f}^T[\sum_\ell\mathbf{U}_{M_o}(\ell)\mathbf{U}_{M_o}^H(\ell)]\mathbf{f}\\ &-\pi_b(\mathbf{f}^T\mathbf{U}_{M_o}(0)\mathbf{f})^2+\mathbf{f}^T\mathrm{E}[\boldsymbol{\epsilon}_{w,M}(k)\boldsymbol{\epsilon}_{w,M}^H(k))]\mathbf{f}\end{aligned} \tag{86}$$

$$\begin{aligned}\mathrm{E}(e_M^2(k)) &= \pi_b\mathbf{f}^T[\sum_\ell\mathbf{U}_{M_o}(\ell)\mathbf{U}_{M_o}^T(\ell)]\mathbf{f}\\ &-\pi_b(\mathbf{f}^T\mathbf{U}_{M_o}(0)\mathbf{f})^2+\delta(M-2)\mathbf{f}^T\mathrm{E}[\boldsymbol{\epsilon}_{w,M}(k)\boldsymbol{\epsilon}_{w,M}^T(k))]\mathbf{f},\end{aligned} \tag{87}$$

where

$$\begin{aligned}\sum_\ell\mathbf{U}_{M_o}(\ell)\mathbf{U}_{M_o}^H(\ell) &= T\int_\Delta(\sum_k\mathbf{U}_{M_o}(k)e^{-j2\pi fkT})\\ &(\sum_\ell\mathbf{U}_{M_o}^H(\ell)e^{j2\pi f\ell T})df\end{aligned} \tag{88}$$

$$\begin{aligned}\sum_\ell\mathbf{U}_{M_o}(\ell)\mathbf{U}_{M_o}^T(\ell)) &= T\int_\Delta(\sum_k\mathbf{U}_{M_o}(k)e^{-j2\pi fkT})\\ &(\sum_\ell\mathbf{U}_{M_o}^T(\ell)e^{j2\pi f\ell T})df\end{aligned} \tag{89}$$

with

$$\begin{aligned}&\sum_k\mathbf{U}_{M_o}(k)e^{-j2\pi fkT}\\ &= \frac{1}{T}\sum_\ell\mathbf{W}_{M_o}^H(f-\frac{\ell}{T})\mathbf{G}_M(f-\frac{\ell}{T})\\ &= \frac{1}{T}\mathbf{C}_M^d(f)[\sum_\ell\mathbf{G}_M^H(f-\frac{\ell}{T})\mathbf{G}_M(f-\frac{\ell}{T})]\\ &= (\mathbf{I}_{P+1}-\frac{N_0}{\pi_b})\mathbf{C}_M^d(f).\end{aligned} \tag{90}$$

Using

$$\begin{aligned}
&\mathrm{E}[\boldsymbol{\epsilon}_{w,M}(k)\boldsymbol{\epsilon}_{w,M}^H(k))] \\
&= N_0 \int \mathbf{W}_{M_o}^H(f)\mathbf{W}_{M_o}(f)df \\
&= N_0 \int_\Delta \mathbf{C}_M^d(f)[\sum_\ell \mathbf{G}_M^H(f-\frac{\ell}{T})\mathbf{G}_M(f-\frac{\ell}{T})]\mathbf{C}_M^d(f)df \\
&= N_0 T \int_\Delta [\mathbf{C}_M^d(f) - \frac{N_0}{\pi_b}\mathbf{C}_M^d(f)\mathbf{C}_M^d(f)]df \qquad (91)
\end{aligned}$$

and

$$\begin{aligned}
&\mathrm{E}[\boldsymbol{\epsilon}_{w,M}(k)\boldsymbol{\epsilon}_{w,M}^T(k))] \\
&= \delta(M-2)N_0 \int \mathbf{W}_{M_o}^H(f)\mathbf{J}_{2N}\mathbf{W}_{M_o}^*(-f)df \\
&= N_0 T \int_\Delta [\mathbf{C}_M^d(f) - \frac{N_0}{\pi_b}\mathbf{C}_M^d(f)\mathbf{C}_M^d(f)]df \qquad (92)
\end{aligned}$$

where we have used in (92) for $M = 2$, the relations $\mathbf{J}_{2N}\mathbf{G}_M(-f) = \mathbf{G}_M^*(f)$ and $\mathbf{C}_M^{d^*}(-f) = \mathbf{C}_M^d(f)$.

Gathering (91), (88) with (90) in (86), and (92), (89) with (90) in (87), the generic expression of the SINR (33) takes the value (44). For $M = 2$, using $\mathbf{f}^T\mathbf{C}_M^d(f)\mathbf{C}_M^d(f)\mathbf{f} = \mathbf{f}^T\mathbf{C}_M^d(f)\mathbf{C}_M^{d^*}(-f)\mathbf{f} = \|\mathbf{C}_M^d(f)\mathbf{f}\|^2$, (44) reduces to (45). ■

B. Proofs related to the MMSE (s) receivers

1) Proof of (14)*:* The output, at time kT of the filter $\mathbf{w}_M^*(f)$ is given by the SO stationary signal:

$$y_M(k) = u_M(0)b_k + \sum_{\ell\neq k} u_M(k-\ell)b_\ell + n_{w,M}(k), \quad (93)$$

where $u_M(\ell) \overset{\text{def}}{=} \int \mathbf{w}_M^H(f)\mathbf{g}_M(f)e^{j2\pi f\ell T}df$ and $n_{w,M}(k) \overset{\text{def}}{=} \int \mathbf{w}_M^H(f)\mathbf{n}_M(f)e^{j2\pi fkT}df$ where $\mathbf{n}_M(t)$ is falsely assumed SO stationary with power spectral density $\mathbf{R}_{n,M}^0(f)$. Following the same steps as that of the derivation of (77), we get the MSE

$$\begin{aligned}
&\mathrm{MSE} \overset{\text{def}}{=} \mathrm{E}|y_k - b_k|^2 \\
&= \pi_b T \int_\Delta \left|1 - \frac{1}{T}\sum_\ell \mathbf{w}_M^H(f-\frac{\ell}{T})\mathbf{g}_M(f-\frac{\ell}{T})\right|^2 df \\
&+ \int_\Delta \sum_k \mathbf{w}_M^H(f-\frac{k}{T})\mathbf{R}_{n_M}^{(0)}(f-\frac{k}{T})\mathbf{w}_M(f-\frac{k}{T})df, \quad (94)
\end{aligned}$$

whose function in the global integral (94) is classically minimized by $\mathbf{w}_{M_s}(f)$ given by (14). ■

2) Proof of (42) *and* (43)*:* The proof follows the same steps as for the optimal MMSE filter, by replacing $\mathbf{f}^T\mathbf{U}_M(k)$ and $\mathbf{f}^T\boldsymbol{\epsilon}_{w,M}(k)$ in (76) by $\int \mathbf{w}_{M_s}^H(f)\mathbf{G}_M(f)e^{-j2\pi fkT}df = \int c^d(f)\mathbf{g}_M^H(f)[\mathbf{R}_{n,M}^0(f)]^{-1}\mathbf{G}_M(f)e^{-j2\pi fkT}df$ and $\int \mathbf{w}_{M_s}^H(f)\boldsymbol{\epsilon}_M(f)e^{-j2\pi fkT}df$, respectively.

C. Proofs related to the MMSE (sc) receivers

1) Proof of (18)*:* As $\mathbf{x}_{v,M}(t)$, given by (17), is SO stationary, $y_{M_{sc}}(k)$, defined by (23), is also SO stationary. From (31), where b_k and $e_{M_{sc}}(k)$ are uncorrelated, and from $u_{M_{sc}} = T\int_\Delta \mathbf{w}_{M_{sc}}^{d^H}(f)\mathbf{g}_{v,M}^d(f)df$, the MSE = $\mathrm{E}(|b_k - y_{M_{sc}}(k)|^2)$ is given by:

$$\begin{aligned}
&\mathrm{MSE} \\
&= \pi_b|1-u_{M_{sc}}|^2 + \mathrm{E}|e_{M_{sc}}(k)|^2 \qquad (95) \\
&= \pi_b|1-u_{M_{sc}}|^2 + \mathrm{E}|y_{M_{sc}}(k)|^2 - \pi_b|u_{M_{sc}}|^2 \\
&= \mathrm{E}|y_{M_{sc}}(k)|^2 + \pi_b(1 - u_{M_{sc}} - u_{M_{sc}}^*) \\
&= T\int_\Delta \Big[\mathbf{w}_{M_{sc}}^{d^H}(f)\mathbf{R}_{x_{v_M}}^d(f)\mathbf{w}_{M_{sc}}^d(f) \\
&+ \pi_b\left(1 - \mathbf{w}_{M_{sc}}^{d^H}(f)\mathbf{g}_{v_M}^d(f) - \mathbf{w}_{M_{sc}}^{d^T}(f)\mathbf{g}_{v_M}^{d*}(f)\right)\Big]df, \quad (96)
\end{aligned}$$

whose function in the integral (96) is classically minimized by $\mathbf{w}_{M_{sc}}^d(f)$ given by (18) for the frequencies such that $\mathbf{x}_{v,M}^d(f) \neq 0$. ■

2) Proof of (24)*:* Similarly, the output $\mathbf{y}_{M_{sc}}(k)$ of the filter $\mathbf{W}_{M_{sc}}^{d^*}(f)$ is SO stationary and

$$\mathbf{y}_{M_{sc}}(k) = \mathbf{U}_{M_{sc}}\mathbf{b}_k + \mathbf{e}_{M_{sc}}(k), \quad (97)$$

where $\mathbf{U}_{M_{sc}} \overset{\text{def}}{=} \int_\Delta \mathbf{W}_{M_{sc}}^{d^H}(f)\mathbf{G}_{v_M}^d(f)df$ and where $\mathbf{b}_k$ and $\mathbf{e}_{M_{sc}}(k)$ are uncorrelated. This implies that the JMSE = $\mathrm{E}\|\mathbf{b}_k - \mathbf{y}_{M_{sc}}(k)\|^2$ is given by:

$$\begin{aligned}
&\mathrm{JMSE} \\
&= \mathrm{E}\|(\mathbf{U}_{M_{sc}} - \mathbf{I}_{P+1})\mathbf{b}_k\|^2 + \mathrm{E}\|\mathbf{e}_{M_{sc}}(k)\|^2 \\
&= \mathrm{E}\|(\mathbf{U}_{M_{sc}} - \mathbf{I}_{P+1})\mathbf{b}_k\|^2 + \mathrm{E}\|\mathbf{y}_{M_{sc}}(k)\|^2 - \mathrm{E}\|\mathbf{U}_{M_{sc}}\mathbf{b}_k\|^2 \\
&= \mathrm{E}\|\mathbf{y}_{M_{sc}}(k)\|^2 + \pi_b\mathrm{Tr}[(\mathbf{U}_{M_{sc}} - \mathbf{I}_{P+1})(\mathbf{U}_{M_{sc}} - \mathbf{I}_{P+1})^H] \\
&- \pi_b\mathrm{Tr}(\mathbf{U}_{M_{sc}}\mathbf{U}_{M_{sc}}^H) \\
&= T\int_\Delta \mathrm{Tr}[\mathbf{W}_{M_{sc}}^{d^H}(f)\mathbf{R}_{x_{v_M}}^d(f)\mathbf{W}_{M_{sc}}^d(f) \\
&+ \pi_b(\mathbf{I}_{P+1} - \mathbf{W}_{M_{sc}}^{d^H}(f)\mathbf{G}_{v_M}^d(f) - \mathbf{W}_{M_{sc}}^{d^T}(f)\mathbf{G}_{v_M}^{d*}(f))]df \quad (98)
\end{aligned}$$

and is minimized for

$$\mathbf{W}_{M_{sc}}^d(f) = \pi_b[\mathbf{R}_{x_{v_M}}^d(f)]^{-1}\mathbf{G}_{v_M}^d(f), \quad (99)$$

whose first column is $\mathbf{w}_{M_{sc}}^d(f)$ (24). ■

3) Proof of (44) *and* (45)*:* It follows that the derived structured MMSE receiver $\mathbf{w}_{M_{sc}}^d(f)$ gives

$$u_{M_{sc}} = T\int_\Delta \mathbf{g}_{M_{sc}}^{d^H}(f)[\mathbf{R}_{x_{v_M}}^d(f)]^{-1}\mathbf{g}_{M_{sc}}^d(f)df \quad (100)$$

that is real-valued and besides (23) gives:

$$\begin{aligned}
&\mathrm{E}(|y_{M_{sc}}(k)|^2) \\
&\quad = T\int_{\Delta} \mathbf{w}_{M_{sc}}^{d^H}(f)\mathbf{R}_{x_{v_M}}^{d}(f)\mathbf{w}_{M_{sc}}^{d}(f)df \\
&\quad = T\pi_b^2\int_{\Delta} \mathbf{g}_{M_{sc}}^{d^H}(f)[\mathbf{R}_{x_{v_M}}^{d}(f)]^{-1}\mathbf{g}_{M_{sc}}^{d}(f)df \quad (101) \\
&\mathrm{E}(y_{M_{sc}}^2(k)) \\
&\quad = T\int_{\Delta} \mathbf{w}_{M_{sc}}^{d^H}(f)\mathbf{C}_{x_{v_M}}^{d}(f)\mathbf{w}_{M_{sc}}^{d^*}(-f)df \quad (102) \\
&\quad = T\pi_b^2\int_{\Delta} \mathbf{g}_{v_M}^{d^H}(f)[\mathbf{R}_{x_{v_M}}^{d}(f)]^{-1}\mathbf{C}_{x_{v_M}}^{d}(f) \\
&\qquad\qquad [\mathbf{R}_{x_{v_M}}^{d^*}(-f)]^{-1}\mathbf{g}_{v_M}^{d^*}(-f)df. \quad (103)
\end{aligned}$$

Using (100), (101) and (103) in (33), (44) and (45) follow for $M = 1$ and $M = 2$, respectively. ■

REFERENCES

[1] B. Picinbono and P. Chevalier, "Widely linear estimation with complex data," *IEEE Trans. Signal Process.*, vol. 43, no. 8, pp. 2030-2033, Aug. 1995.

[2] B. Picinbono, "On circularity," *IEEE Trans. Signal Process.*, vol. 42, no. 12, pp. 3473-3482, Dec 1994.

[3] Z. Ding and G. Li, "Single-Channel blind equalization for GSM cellular systems", *IEEE J. Sel. Areas Commun.*, vol. 16, no. 8, pp. 1493-1505, Oct. 1998.

[4] G. Gelli, L. Paura, and A.M. Tulino, "Cyclostationarity-based filtering for narrow-band interference suppression in direct-sequence spread spectrum systems", *IEEE J. Selected Areas Commun.*, vol 6, no. 9, pp. 1747-1755, Dec. 1998.

[5] G. Gelli, L. Paura, and A. R. P. Ragozini, "Blind widely linear multiuser detection," *IEEE Commun. Lett.*, vol. 4, pp. 187-189, Jun. 2000.

[6] S. Buzzi, M. Lops, and A. M. Tulino, "A new family of MMSE multiuser receivers for interference suppression in DS/CDMA systems employing BPSK modulation," *IEEE Trans. Commun.*, vol. 49, pp. 154-167, Jan. 2001.

[7] A. M. Tulino and S. Verdu, "Asymptotic analysis of improved linear receivers for BPSK-CDMA subject to fading," *IEEE J. Sel. Areas Commun.*, vol. 19, pp. 1544-1555, Aug. 2001.

[8] S. Buzzi, M. Lops, and A. M. Tulino, "A generalized minimum-mean-output-energy for CDMA systems with improper MAI," *IEEE Trans Inf. Theory*, vol. 48, pp. 761-767, Mar. 2002.

[9] S. Buzzi and M. Lops, "Performance analysis for the improved linear multiuser detectors in BPSK-modulated DS-CDMA systems," *IEEE Trans. Commun.*, vol. 51, pp. 37-42, Jan. 2003.

[10] R. Schober, W. Gerstacker, and L. Lampe, "Data-aided and blind stochastic gradient algorithms for widely linear MMSE MAI suppression for DS-CDMA," *IEEE Trans. Signal Process.*, vol. 52, pp. 746-756, March 2004.

[11] Y. C. Yoon and H. Leib, "Maximizing SNR in improper complex noise and applications to CDMA," *IEEE Commun. Lett.*, vol. 1, pp. 5-8, Jan. 1997.Mar. 2004.

[12] M. Konrad and W.H. Gerstacker, "Interference robust transmission for the downlink of an OFDM-Based mobile communications system," *EURASIP J. Wireless Commun. Netw.*, vol. 2008.

[13] N. Song, R.C. De Lamare, M. Haardt, and M. Wolf, "Adaptive widely linear reduced-rank interference suppression based on the multistage Wiener filter estimation", *IEEE Trans.Signal Process.*, vol. 60, no. 8, pp. 4003-4016, Aug. 2012.

[14] D. Mattera, L. Paura, and F. Sterle, "Widely linear MMSE equalizer for MIMO linear time-dispersive channel," *Electronic Letters*, vol. 39, no. 20, pp. 1481-1482, Oct. 2003.

[15] S. Buzzi, M. Lops, and S. Sardellitti, "Widely linear reception strategies for layered space-time wireless communications," *IEEE Trans. Signal Process.*, vol. 54, no. 6, pp. 2252-2262, Jun. 2006.

[16] P. Chevalier and F. Dupuy, "Widely linear Alamouti receivers for the reception of real-valued signals corrupted by interferences - The Alamouti SAIC/MAIC concept", *IEEE Trans. Signal Process.*, vol. 59, no. 7, pp. 3339-3354, July 2011.

[17] A. Mirbagheri, K.N. Plataniotis and S. Pasupathy, "An enhanced Widely Linear CDMA receiver with OQPSK modulation", *IEEE Trans. Commun.*, vol. 54, no. 2, pp. 261-272, Feb. 2006.

[18] H. Trigui and D.T.M. Slock, "Performance bounds for cochannel interference cancellation within the current GSM standard," *Signal Proccess., Elsevier*, vol. 80, pp. 1335-1346, 2000.

[19] P. Chevalier and F. Pipon, "New insights into optimal widely linear array receivers for the demodulation of BPSK, MSK and GMSK signals corrupted by non circular interferences - Application to SAIC," *IEEE Trans. Signal Process.*, vol. 54, no. 3, pp. 870-883, March 2006.

[20] R. Meyer, W.H. Gerstacker, R. Schober, and J.B. Huber, "A single antenna interference cancellation algorithm for increased GSM capacity", *IEEE Trans. Wireless Commun.*, vol. 5, no. 7, pp. 1616-1621, July 2006.

[21] J.C. Olivier and W. Kleynhans, "Single antenna interference cancellation for synchronised GSM networks using a widely linear receiver," *IET Commun.*, vol. 1, no. 1, pp. 131-136, 2007.

[22] M. Austin, "SAIC and synchronised networks for increased GSM capacity," in 3G Americas SAIC Working Group, Sep. 2003.

[23] A. Mostapha, R. Kobylinski, I. Kostanic, and M. Austin, "Single antenna interference cancellation (SAIC) for GSM networks", *IEEE Proc. Vehicular Technology Conf.*, vol. 2, pp. 1089-1093, Oct. 2004.

[24] M.G. Vutukuri, R. Malladi, K. Kuchi, and R.D. Koilpillai, "SAIC receiver algorithms for VAMOS downlink transmission," *Proc. 8th Int. Symp. Wireless Commun. Syst.*, pp. 31-35, Aug. 2011.

[25] W.H. Gerstacker, R. Schober, R. Meyer, F. Obernosterer, M. Ruder, and H. Kalveram, "GSM/EDGE: A mobile communications system determined to stay," *Inter. Journal Elec. Commun.*, vol. 65, pp. 694-700, 2011.

[26] M. Ruder, R. Meyer, F. Obernosterer, H. Kalveram, R. Schober, and W.H. Gerstacker, "Receiver concepts and resource allocation for OSC downlink transmission," *IEEE Trans. Wireless Commun.*, vol. 13, no. 3, pp. 1568-1581, March 2014.

[27] D. Molteni and M. Nicoli, "Joint OSC receiver for evolved GSM/EDGE," *IEEE Trans. Wireless Commun.*, vol. 12, no. 6, pp. 2608-2619, June 2013.

[28] W. Deng, Z. Li, Y. Xia, K. Wang, and W. Pei, "A Widely linear MMSE Anti-Collision method for multi-antenna RFID readers," *IEEE Commun. Letters*, vol 23, no. 4, pp. 664-647, Aug. 2019.

[29] R. Gui, N.M. Balasubramanya, and L. Lampe, "Connectivity performance evaluation for grant-free narrowband IoT with widely linear receivers," *IEEE Internet of Things Journal*, vol 7, no. 10, pp. 10562-10572, Oct. 2020.

[30] D.J. Nelson and J.R. Hopkins, "Coherent demodulation of AIS-GMSK signals in co-channel interference," *IEEE Asilomar Conf. on Circuits, Systems and Computers*, Nov. 2011.

[31] G.M. Swetha, K. Hemavathy, S. Natarajan, and V. Sambasiva, "Overcome message collisions in satellite automatic ID systems, *Microwave and RF, Systems*, May. 2018.

[32] O. Cherrak, H. Ghennioui, N. Thirion-Moreau, and E.H. Abarkan, "Blind separation of complex-valued satellite-AIS data for maritime surveillance : a spatial quadratic time-frequency domain approach," *International Journal of Electrical and Computer Engineering (IJECE)*, pp. 1732-1741, June. 2019.

[33] M. Bavand and S.D. Blostein, "User selection and multiuser widely linear precoding for one-dimensional signalling," *IEEE Trans. Vehicular Technology*, vol. 67, no. 12, pp. 11642-11653, Dec. 2018.

[34] S. Javed, O. Amin, B. Shihada, and M.S. Alouini, "A journey from improper Gaussian signaling to asymetric signaling," *IEEE Commun. Surveys and Tutorials*, vol. 22, no. 3, pp. 1539-1591, Third Quarter 2020.

[35] D. Tong, Y. Ding, Y. Liu, and Y. Wang, "A MIMO-NOMA framework with complex-valued power coefficients," *IEEE Trans. Vehicular Technology*, vol. 68, no. 3, pp. 2244?-259, March 2019.

[36] J.C. De Luna Ducoing, N. Yi, Y. Ma, and R. Tafazolli, "Using real constellations in fully-and over loaded large MU-MIMO systems with simple detection", *IEEE Wireless Commun. Letters*, vol. 5, no. 1, pp. 92-95, Feb. 2016.

[37] K.P. Valavanis and G.J. Vachtsevanos, *Handbook of Unmanned Aerial Vehicles*, New-York, NY, USA: Springer, 2015.

[38] Y. Zeng, R. Zhang, and T.J. Lim, "Wireless Communications with unmanned aerial vehicles: Opportunities and challenges", *IEEE Commun. Mag.*, vol. 54, no. 5, pp. 36-42, May 2016.

[39] *Command and Control (C2) Data Link Minimum Operational Performance Standards (MOPS) (Terrestrial)*," Document RTCA-DO-362, RTCA Std., 2016.

[40] D. Darsena, G. Gelli, I. Iudice, and F. Verde, "Equalization techniques of control and non-payload communication links for unmanned aerial vehicles," *IEEE Access*, vol. 6, pp. 4485-4496, 2018.

[41] B. Farhang-Boroujeny and R. Kempter, "Multicarrier communication techniques for spectrum sensing and communication in cognitive radios," *IEEE Commun. Mag.*, vol. 46, no. 4, pp. 80-85, Apr. 2008.

[42] D. Chen, Y. Tian, D. Qu, and T. Jiang, "OQAM-OFDM for wireless communications in future internet of things: a survey on key technologies and challenges," *IEEE Internet of Things Journal*, vol. 5, no. 5, pp. 3788-3809, Oct. 2018.

[43] M. Caus and A.I. Perez-Neira, "Comparison of linear and widely linear processing in MIMO-FBMC systems," in *Proc. Int. Symp. Wireless Commun. Syst.*, pp. 21-25, Ilmenau, (Germany), Aug. 2013.

[44] M. Caus and A.I. Perez-Neira, "Multi-stream transmission for highly frequency-selective channels in MIMO-FBMC/OQAM systems," *IEEE Trans. Signal Process.*, vol. 62, no. 4, pp. 786-796, Feb. 2014.

[45] Y. Chen and M. Haardt, "Widely linear processing in MIMO FBMC/OQAM systems," in *Proc. Int. Symp. Wireless Commun. Syst.*, pp. 743-747, Ilmenau, (Germany), Aug. 2013.

[46] S. Josilo, M. Narandzic, S. Tomic, and S. Nedic, "Widely linear filtering based kindred CCI suppression in FBMC waveforms", in *Proc. Int. Symp. Wireless Commun. Syst.* Barcelona (Spain), Aug. 2014.

[47] A. Ishaque and G. Ascheid, "Widely linear receivers for SMT systems with TX/RX frequency-selective I/Q imbalance", in *Proc. Int. Symp. Personal, Indoor Mobile Radio Commun.*, pp. 800-805, 2014.

[48] P. Chevalier, R. Chauvat, and J.-P. Delmas, "Enhanced widely linear filtering to make quasi-rectilinear signals almost equivalent to rectilinear ones for SAIC/MAIC," *IEEE Trans. Signal Proces.*, vol. 66, no. 6, pp. 1438-1453, March 2018.

[49] P. Chevalier, R. Chauvat, and J.-P. Delmas, "Widely linear FRESH receivers for cancellation of data-like rectilinear and quasi-rectilinear Interference with frequency-offsets", *Signal Processing*, vol 188, pp. 1-13, 108171, Nov., 2021.

[50] P. Chevalier, J.-P. Delmas, and R. Lamberti, "New insights into widely linear MMSE receivers for communication networks using data-like rectilinear or quasi-rectilinear signals - Part II: Three-input receivers", *IEEE Trans. Vehicular Technology* submitted, Nov. 2023.

[51] W.H. Gerstacker, R. Schober, and A. Lampe, "Receivers with widely linear processing for frequency-selective channels", *IEEE Trans. Commun.*, vol. 51, no. 9, pp. 1512-1523, Sept. 2003.

[52] P.A. Laurent, "Exact and approximate construction of digital phase modulations by superposition of amplitude modulated pulses (AMP)", *IEEE Trans. Commun.*, vol. 34, no. 2, pp. 150-160, Feb. 1986.

[53] J.G. Proakis, *Digital Communications*, Mc Graw Hill Series in Electrical and Computer Engineering, 4th Ed., 2001.

[54] W.A. Gardner, W.A. Brown, and C-K. Chen, "Spectral correlation of modulated signals: Part II - Digital modulation", *IEEE Trans. commun.*, vol. 35, no. 6, pp. 595-601, June 1987.

[55] P. Gournay and P. Viravau, "Corrélation spectrale théorique des modulations CPM, Partie I: Résultat analytique pour les modulations CPFSK à 2 états (1-Rec)", *Annals of Telecom.*, vol 53, no. 7-8, pp. 267-278, 1998.

[56] D. Vucic and M. Obradovic, "Spectral correlation evaluation of MSK and offset QPSK modulation", *Signal Processing*, vol 78, pp. 363-367, 1999.

[57] P. Balaban and J. Sack, "Optimum diversity combining and equalization in digital transmission with applications to cellular mobile radio - Part I: theoretical considerations", *IEEE Trans. commun.*, vol. 40, no. 5, pp. 885-894, May 1992.